U.S. Department
of Transportation
Federal Railroad
Administration

Office of Research,
Development and Technology
Washington, DC 20590

Load Shedding - Phase II & III: Concept Development and Prototype Design for Passenger Rail Equipment

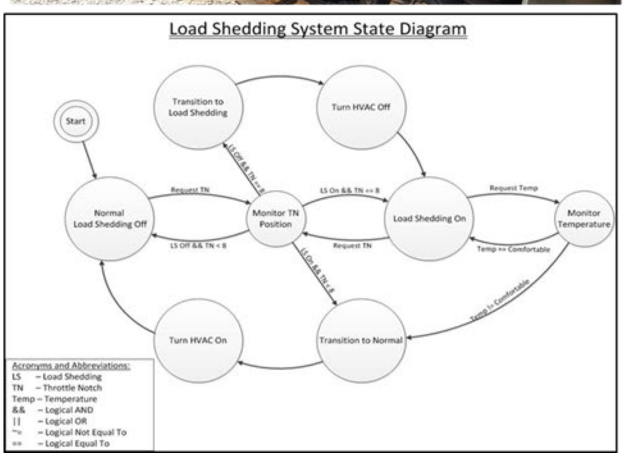

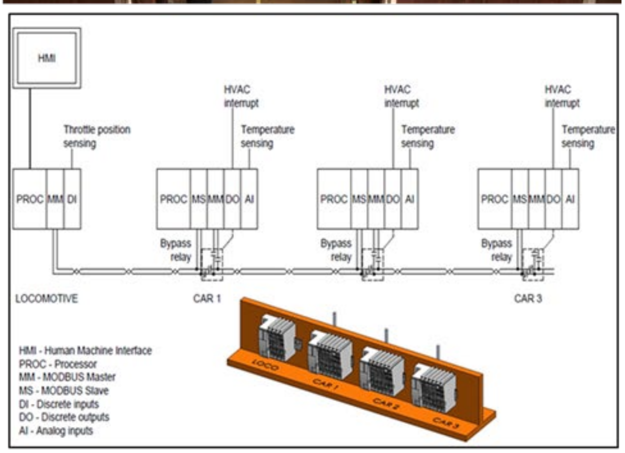

DOT/FRA/ORD-20/30

Final Report | July 2020

REPORT DOCUMENTATION PAGE

Form Approved
OMB No. 0704-0188

1. REPORT DATE *(DD-MM-YYYY)*
Published: July 2020

2. REPORT TYPE
Technical Report

3. DATES COVERED *(From - To)*
July 13, 2017- December 11, 2019

4. TITLE AND SUBTITLE
Load Shedding - Phase II & III: Concept Development and Prototype Design for Passenger Rail Equipment

5a. CONTRACT NUMBER
DTFR53-12-D-00004L

5b. GRANT NUMBER

5c. PROGRAM ELEMENT NUMBER

6. AUTHOR(S)
Anuradha Guntaka (0000-0003-1253-1127), Ken L. Martin (0000-0002-0346-3954), Som P. Singh (0000-0002-6076-6839)

5d. PROJECT NUMBER

5e. TASK NUMBER
DTFR5317F00736

5f. WORK UNIT NUMBER

7. PERFORMING ORGANIZATION NAME(S) AND ADDRESS(ES)
Sharma & Associates, Inc.
100 W. Plainfield Road
Countryside, IL 60525

8. PERFORMING ORGANIZATION REPORT NUMBER

9. SPONSORING/MONITORING AGENCY NAME(S) AND ADDRESS(ES)
U.S. Department of Transportation
Federal Railroad Administration
Railroad Policy and Development
Office of Research, Development and Technology
Washington, DC 20590

10. SPONSOR/MONITOR'S ACRONYM(S)

11. SPONSOR/MONITOR'S REPORT NUMBER(S)

12. DISTRIBUTION/AVAILABILITY STATEMENT
This document is available to the public through the FRA website.

13. SUPPLEMENTARY NOTES

14. ABSTRACT
An investigation occurred by Sharma & Associates, Inc. (SA) of the feasibility of temporarily shedding electrical demand associated with passenger car heating ventilation and air conditioning (HVAC) systems during periods of peak traction demand, with the goal of right-sizing the main engine on a passenger locomotive. Architecture of a concept to monitor the load shedding demand at the locomotive was developed. The necessary MODBUS remote terminal unit (RTU) components for the communication and control were identified, procured and tested in the laboratory to confirm the functionality of the concept. Prototyping and field testing of the concept is recommended.

15. SUBJECT TERMS
Head-end power, heating ventilation and air condition, HVAC, load shedding, locomotive, MODBUS RTU, remote terminal unit, passenger, Programmable Logic Controller, PLC, rolling stock

16. SECURITY CLASSIFICATION OF: a. REPORT	b. ABSTRACT	c. THIS PAGE	17. LIMITATION OF ABSTRACT	18. NUMBER OF PAGES	19a. NAME OF RESPONSIBLE PERSON
				53	19b. TELEPHONE NUMBER *(Include area code)*

Standard Form 298 (Rev. 8/98)
Prescribed by ANSI Std. Z39.18

METRIC/ENGLISH CONVERSION FACTORS

ENGLISH TO METRIC

LENGTH (APPROXIMATE)

1 inch (in)	=	2.5 centimeters (cm)
1 foot (ft)	=	30 centimeters (cm)
1 yard (yd)	=	0.9 meter (m)
1 mile (mi)	=	1.6 kilometers (km)

AREA (APPROXIMATE)

1 square inch (sq in, in^2)	=	6.5 square centimeters (cm^2)
1 square foot (sq ft, ft^2)	=	0.09 square meter (m^2)
1 square yard (sq yd, yd^2)	=	0.8 square meter (m^2)
1 square mile (sq mi, mi^2)	=	2.6 square kilometers (km^2)
1 acre = 0.4 hectare (he)	=	4,000 square meters (m^2)

MASS - WEIGHT (APPROXIMATE)

1 ounce (oz)	=	28 grams (gm)
1 pound (lb)	=	0.45 kilogram (kg)
1 short ton = 2,000 pounds (lb)	=	0.9 tonne (t)

VOLUME (APPROXIMATE)

1 teaspoon (tsp)	=	5 milliliters (ml)
1 tablespoon (tbsp)	=	15 milliliters (ml)
1 fluid ounce (fl oz)	=	30 milliliters (ml)
1 cup (c)	=	0.24 liter (l)
1 pint (pt)	=	0.47 liter (l)
1 quart (qt)	=	0.96 liter (l)
1 gallon (gal)	=	3.8 liters (l)
1 cubic foot (cu ft, ft^3)	=	0.03 cubic meter (m^3)
1 cubic yard (cu yd, yd^3)	=	0.76 cubic meter (m^3)

TEMPERATURE (EXACT)

[(x-32)(5/9)] °F = y °C

METRIC TO ENGLISH

LENGTH (APPROXIMATE)

1 millimeter (mm)	=	0.04 inch (in)
1 centimeter (cm)	=	0.4 inch (in)
1 meter (m)	=	3.3 feet (ft)
1 meter (m)	=	1.1 yards (yd)
1 kilometer (km)	=	0.6 mile (mi)

AREA (APPROXIMATE)

1 square centimeter (cm^2)	=	0.16 square inch (sq in, in^2)
1 square meter (m^2)	=	1.2 square yards (sq yd, yd^2)
1 square kilometer (km^2)	=	0.4 square mile (sq mi, mi^2)
10,000 square meters (m^2)	=	1 hectare (ha) = 2.5 acres

MASS - WEIGHT (APPROXIMATE)

1 gram (gm)	=	0.036 ounce (oz)
1 kilogram (kg)	=	2.2 pounds (lb)
1 tonne (t)	=	1,000 kilograms (kg)
	=	1.1 short tons

VOLUME (APPROXIMATE)

1 milliliter (ml)	=	0.03 fluid ounce (fl oz)
1 liter (l)	=	2.1 pints (pt)
1 liter (l)	=	1.06 quarts (qt)
1 liter (l)	=	0.26 gallon (gal)
1 cubic meter (m^3)	=	36 cubic feet (cu ft, ft^3)
1 cubic meter (m^3)	=	1.3 cubic yards (cu yd, yd^3)

TEMPERATURE (EXACT)

[(9/5) y + 32] °C = x °F

QUICK INCH - CENTIMETER LENGTH CONVERSION

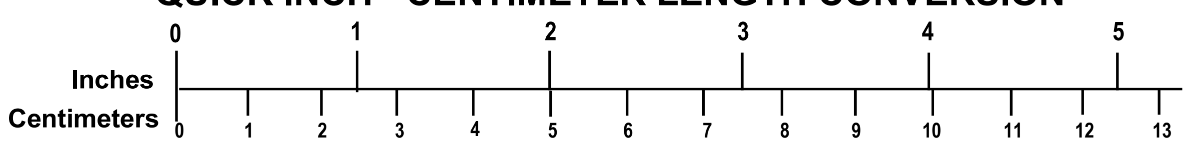

QUICK FAHRENHEIT - CELSIUS TEMPERATURE CONVERSIO

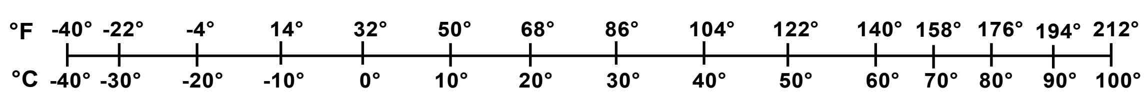

For more exact and or other conversion factors, see NIST Miscellaneous Publication 286, Units of Weights and Measures. Price $2.50 SD Catalog No. C13 10286

Updated 6/17/98

Contents

Executive Summary ... 1

1. Introduction ... 3
   - 1.1. Background ... 3
   - 1.2. Load Shedding in Industrial Applications ... 4
   - 1.3. Scope and Objective ... 5
   - 1.4. Overall Approach ... 5
   - 1.5. Organization of the Report ... 6
2. Temperature Testing of Coaches for Interior Heating and Cooling Behavior ... 7
   - 2.1. PRIIA Passenger Comfort Temperature Limits ... 7
   - 2.2. Field Tests on Passenger Coaches for Thermal Model Validation ... 7
   - 2.3. Bi-level Coach Temperature Testing ... 8
   - 2.4. Single Level Coach Temperature Testing ... 13
3. Thermal Model Validation ... 17
   - 3.1. Computational Fluid Dynamics Model ... 17
4. Load Shedding Monitoring System Concept ... 23
   - 4.1. Programmable Logic Controller (PLC) Modbus RTU ... 23
5. Network Architecture ... 24
6. Load Shedding Hardware ... 25
   - 6.1. Human Machine Interface ... 25
   - 6.2. Passenger Car Hardware ... 25
   - 6.3. HVAC Interface ... 25
   - 6.4. Network Hardware ... 26
7. Load Shedding Software ... 27
   - 7.1. Communication Protocol ... 27
8. Proof-of-Concept Testbed ... 31
9. Conclusion ... 32
10. References ... 33

Appendix A. Passenger Coach Specifications ... 34

Appendix B. Properties of Materials Used in Analysis ... 36

Appendix C. Computation of Heat Transfer Through Solid Layers Using One-Dimensional Model ... 37

Abbreviations and Acronyms ... 46

Illustrations

Figure 2-1. Bi-level passenger coach selected for temperature testing 8

Figure 2-2. Instrumentation of the bi-level passenger coach 9

Figure 2-3. Thermocouple locations on the first and second floors of the bi-level passenger coach 10

Figure 2-4. Thermocouple used for temperature measurement 11

Figure 2-5. Temperature rise time history measured on bi-level coach—as recorded 12

Figure 2-6. Temperature rise time history on bi-level coach—offset to lower PRIIA bound 12

Figure 2-7. Single level passenger coach selected for temperature testing 13

Figure 2-8. Instrumentation of the single level passenger coach 14

Figure 2-9. Thermocouple locations in the single level passenger coach.................................... 14

Figure 2-10. Temperature rise time history measured on single level coach—as recorded 15

Figure 2-11. Temperature rise time history measured on single level coach—offset to lower PRIIA bound 16

Figure 3-1. Finite element model (half coach) including walls, floor, roof, seats, and windows (260,956 nodes, 547,959 elements) 18

Figure 3-2. Finite element model for air volume only (233,338 nodes, 1,172,792 elements) seats shown for location.. 18

Figure 3-3. Finite element mesh details for solid material 19

Figure 3-4. Finite element mesh details for air volume 19

Figure 3-5. Air volume CFD model predicted temperature in the interior at the start (left, 70.0 °F) and after 1 minute (right, 70.9 °F) 20

Figure 3-6. Air volume CFD model predicted temperature in the interior at the end of 2 minutes (left, 71.5 °F) and 3 minutes (right, 72.4 °F) 20

Figure 3-7. Air volume CFD model predicted temperature in the interior at the end of 4 minutes (left, 73.2 °F) and 5 minutes (right, 73.9 °F) 21

Figure 3-8. Air volume CFD model predicted temperature in the interior at the end of 6 minutes (left, 74.6 °F) and 7 minutes (right, 77.9 °F) 21

Figure 3-9. Air volume CFD model predicted temperature in the interior at the end of 8 minutes (left, 76 °F) and 9 minutes (right, 76.6 °F) 22

Figure 3-10. Air volume CFD model predicted temperature in the interior at the end of 10 minutes (left, 77.3 °F) and 11 minutes (right, 77.9 °F)... 22

Figure 5-1. Modbus RTU network diagram 24

Figure 7-1. Load shedding state diagram... 27

Figure 8-1. Load-shedding concept testbed 31

Tables

Table 1. Variable explanation 28
Table 2. COMMAND variable bit-fields 29
Table 3. Modbus message data field table for master reads 29
Table 4. Modbus message data field table for master writes 30

Executive Summary

Right-sizing a locomotive diesel engine for various load demands, including traction and passenger comfort, is beneficial from multiple perspectives. It is feasible to temporarily shed electrical demand associated with passenger car heating ventilation and air condition (HVAC) systems during periods of peak traction needs, with the goal of right-sizing the main engine on a passenger locomotive. Between July 31, 2017, and December 11, 2019, the Federal Railroad Administration funded Sharma & Associates, Inc. (SA) to validate concepts developed during the Phase I feasibility study in Countryside, IL. This phase of research focused on validating the computer models developed in Phase I and the development of the architecture for a load-shedding system for passenger rail.

To validate the observations of the results of the Phase I effort, temperature tests were conducted on two passenger coaches: a single level coach and a bi-level coach. The tests showed that the temperature in the interior of a coach can rise above the Passenger Rail Investment and Improvement Act (PRIIA) specification for passenger rail car [1] comfort limits within 10 minutes of an HVAC shutoff resulting from the load-shedding initiation by the locomotive engineer. Phase I simulation showed that 10 minutes is the optimal load-shedding period required under peak engine power demand (notch 7 or 8) needed to maintain desired maximum operating train speed.

System architecture for communication and control of the load-shedding concept was also developed in this phase of the research. The hardware components for the system were identified and procured as off-the-shelf items. Through a literature search, an appropriate communication protocol entitled Modbus Remote Terminal Unit (Modbus RTU), was identified and the associated software was acquired.

A four-node network testbed was set up in the lab representing a 4-vehicle train: one locomotive and three passenger coaches. The locomotive load-shedding needs requiring a HVAC shutdown and restart were emulated via a laptop.

The laboratory testing of the concept verified that the communication modules can dynamically and automatically configure themselves, regardless of car position and orientation. This was an essential requirement for this system, so that load shedding system initialization does not impede normal train building operations.

Additional load-shedding functionality was also developed and tested using the testbed to confirm that the software functioned as laid out in concept architecture, including automatic train building.

Based on the simulation and measurement of temperature inside a passenger coach, a computational fluid thermodynamics model was validated for its prediction of temperature when the HVAC is turned off during load shedding. Such predictions can be used to set load-shedding boundaries for the target equipment.

A finite element analysis of a typical single passenger coach was carried out for cooling conditions to determine the maximum length of time the HVAC system could be deactivated and maintain the interior air temperature within the PRIIA comfort bounds of 72–76 °F for the summer. The PRIIA specifications were chosen because it is more likely that new cars and locomotives will be outfitted with load-shedding equipment.

The thermal analytical model simulations showed that it can predict temperature rise in the interior of a passenger coach when HVAC system is shut down under load shedding demand. The model predictions for the temperature rise and the associated time for the temperature increase were in close agreement with the field data collected in Phase II of the project.

An additional effort is recommended to implement the developed load-shedding concept on a demonstration train as a validation of the assumptions and results observed so far.

1. Introduction

Between July 31, 2017, and December 31, 2019, the Federal Railroad Administration (FRA) contracted with Sharma & Associates, Inc. (SA) to conduct research on validating concepts for load shedding of passenger locomotive engine for improved efficiency. This work builds upon previous research that investigated the feasibility of load shedding for passenger locomotives. Research efforts under a prior phase of the project established that the concept of load shedding does not compromise either the train performance or passenger comfort [2]. This was accomplished through an analytical simulation of the train operations and a thermal analysis of a passenger coach operated over a long-distance route with sufficient grade changes to require maximum traction operation periodically.

1.1. Background

Traditionally, locomotives used in passenger service employ a separate engine to supply electricity to power comfort features, i.e., heating, ventilation and air conditioning (HVAC), lighting, etc. on the coupled passenger coach consist. Commonly referred to as head-end power (HEP) or hotel power systems, these units generally consist of a diesel engine and associated alternator that supplies 480 volt alternating currents (VAC), 3-phase (50-60 Hz) power. Some variants have included systems where the HEP alternator is driven mechanically by the main engine (prime mover), as well as some newer systems in which hotel power is taken from the main alternator and conditioned using the appropriate power electronics to supply the coaches.

In most conventional passenger locomotives, HEP output and demand has been about 600–700 hp, with newer locomotive specifications requiring even more HEP capacity. For example, the Passenger Rail Investment and Improvement Act (PRIIA) locomotive specifications have a requirement for 800 hp HEP. Even among modern higher speed/high horsepower locomotives, that is a notable portion of the overall locomotive power output.

Some newer locomotives have tended to move away from the traditional separate HEP engine model and instead use a larger prime mover that supplies both traction and HEP needs. Reasons for combining the power generation capacity include fuel efficiency concerns, as well as the need for increased traction power to meet higher top speed requirements. Additionally, the HEP engine will need to meet the U.S. Environmental Protection Agency tier 4 emissions requirements resulting in added complexity of locomotive system design and packaging.

The horsepower needs of modern locomotives are driven by:

1. Traction requirements based on top speed, acceleration, trailing load, grades, etc.
2. HEP requirements based on the number of passenger coaches, heating/cooling requirements, passenger convenience such as power ports, displays and Wi-Fi, etc.
3. Auxiliary power needs for blower motors, radiator fans, control electronics, cab comfort, etc. These demands are usually supplied by an auxiliary generator that is driven by the prime mover. Auxiliary power requirements are generally lower, peaking at about 200 hp, compared to the much higher traction and HEP power requirements.

1.2. Load Shedding in Industrial Applications

Load shedding in an industrial facility is utilized to manage situations when the demand for electrical power is greater than the supply, whether self-generated or provided by an external source. When load shedding is needed, some of the demand for electricity is temporarily removed in a controlled fashion to avoid exceeding the current supply. The need to shed some of the electrical demand can occur due to several different reasons, such as capacity limitations, supply disturbances and energy savings due to the higher cost of peak power supply.

Load shedding for capacity and disturbance issues are critical to protect the plant's equipment and minimize downtime. Load shedding and balancing during peak power usages can result in substantial energy cost savings.

During normal operation, the system load is equal to or less than the generated load. The system is in a stable state and operates at a normal supply frequency. Slow load increases and minor overloads are monitored by governors and will respond to the speed change, and unused capacity will be used to equalize the system. Large, rapid fluctuations in generation capacity impact the system resulting in a load imbalance and fast frequency decline.

There are a few different approaches to shedding the electrical load as outlined below.

1.2.1. Local Control

Most operations use a Programmable Logic Controller (PLC) installed on each electrical load unit to control the load shedding process. The system is programmed based on system load versus generated load using maximum and minimum frequency conditions. The PLC's are programmed to initiate a signal to trip the breaker. Breaker trips are done in a specific preset sequence, if a multiple-stage shutdown is required, to shed the local load. This sequence continues until the frequency becomes normal and stable. Time response between system detection and load shedding in larger systems is critical. In this system, the load shedding is done in the same order every time unless the PLC's are reprogrammed for a different sequence. The PLC reprogramming must be done locally, at each PLC. This would typically be utilized when there are only one or two large loads that would be dropped in the event of a power supply issue or demand control requirement. Local control type systems are reactive systems where action is taken after a problem is detected. Loads will continue to shut down until there is no longer an overload detected at the supply.

1.2.2. Intelligent System Control

Intelligent system control incorporates servers to continuously monitor and control the electrical load. The server passes the trigger signal to the PLC to initiate the load shedding sequence. A database of sequences of loads to be shed is compiled from all possible combinations, based on various levels of power loss. Substantial efficiencies over only PLC control is achieved using this technique since the server processing can drop loads intelligently. For instance, if the system is only slightly overloaded, the server can shut down only the smallest load that will correct the overload situation, rather than shutting devices down in a predefined sequence. Intelligent system control is a reactive control methodology.

Another benefit offered by executing the required calculations at the server level is the ability to update load priority lists and logic from one console. This reduces the downtime required for updating the logic and eliminates removing and reprogramming the PLCs whenever a logic change has to be made. There is usually a fail-safe or default priority table written to the PLCs which is used in the event of server failure.

1.2.3. Interruptible Load Shedding

Under this approach, the utility will negotiate a contract with the high-demand industrial consumers to curtail usage during peak demand times, typically in the summer months. The peak demand times may be defined in the contract, or the utility may contact the consumer shortly before a peak demand may occur. The consumer will then begin shedding loads using a scheme such as intelligent logic control to meet the curtailed supply. This process can involve manually disconnecting loads, or intelligent PLC and/or PC based systems to manage the load environment. With this type of system, prior knowledge of an overload condition exists, therefore, the load can be managed proactively.

The passenger locomotive load application is most closely aligned with the interruptible load shedding approach, since the goal is to shed loads only during times of peak power demand, which occur when maximum tractive effort is required during acceleration or maintaining speed on ascending grades.

Preliminary evaluation of the concept of temporarily shedding electrical demand associated with passenger car HVAC systems during periods of peak traction needs, with the goal of right-sizing the main engine on a passenger locomotive, indicated the technical and economic feasibility of the concept.

1.3. Scope and Objective

The research project consists of furthering the load-shedding concept to prototype components and in-lab testing of the components and communication protocol. The overall scope under the effort included the following:

- Temperature testing of typical single-level and bi-level passenger coaches
- Validation of the computational fluid dynamics (CFD) model of a single-level passenger coach using the data from temperature testing
- Develop the architecture of the load-shedding concept and develop details of its hardware and software elements
- Testing of the concept components and communication protocol in lab as developed in the proposed architecture

1.4. Overall Approach

The overall approach of the work was to pursue the analytical work for the thermal validation and the development of architecture for communication and control in parallel. This was facilitated by the fact that the thermal validation work involved field testing of selected passenger cars followed up by the modeling and finite element analysis of the thermal heating and cooling of car interior using CFD modeling. The development of architecture for communication and control required a team with a different skill and experience and thus could be carried out independent of the analysis team.

1.5. Organization of the Report

As listed in Section 1.2, the effort was focused on three major tasks: CFD thermal model validation, architectural layout of the communication and control systems and development of communication and control hardware and software, and, finally, functional testing of the concept in a laboratory testbed.

Section 2 discusses the efforts to access passenger coaches, instrumentation for temperature testing, and the conducting of cooling and natural heating after the air conditioning shutoff to determine the time record when the interior temperature reaches the upper comfort limits.

Section 3 includes the validation of the finite element model of the passenger car. The validation is carried out based on testing of a single level and a bi-level coach. This finite element model is more comprehensive than the one used to assess the thermal performance of the car in Phase I.

Section 4 describes the suitable PLC based on the Modbus Remote Terminal Unit (Modbus RTU), a de facto standard communication protocol and is now a commonly available means of connecting industrial electronic devices.

Section 5 lays out the proposed system architecture and describes the Modbus RTU network functionality as relating to the locomotive and coaches in the train.

Sections 6 and 7 describes the recommended hardware and the associated software required per the system architecture described in Section 5.

Section 8 includes the testing results of the system created as a 4-node mockup of a train made of a locomotive and three passenger cars.

A summary of the project efforts is included in Section 9.

Additional information is found in Appendices A through C.

2. Temperature Testing of Coaches for Interior Heating and Cooling Behavior

Air conditioners typically require a few minutes of down time after shutdown before the system can be restarted. Modern thermostats have the timer built into the logic of the programming. Technically there is no difference between the thermostat deactivating the HVAC and a remote unit deactivating the HVAC. The only requirement is that the system restart timer be activated when the remote shutoff is in effect. Temporarily deactivating the HVAC inside passenger coaches to obtain maximum traction on the locomotives may result in the interior temperature of the passenger coaches to move into a range of discomfort.

2.1. PRIIA Passenger Comfort Temperature Limits

The PRIIA [1] specifications for passenger coaches include provisions for passenger comfort. These specifications are outlined in Section 10.4 of the PRIIA (2012) and include allowable temperature variations of:

1. Vertical (same floor) [5 °F maximum]
2. Horizontal [±3 °F from the average temperature at that level]
3. Top level to bottom level [4 °F maximum]
4. Seasonal conditions [72–76 °F summer; 68–72 °F winter]

The seasonal conditions listed above are specified for ensuring that the design of the HVAC system can maintain the interior temperature for both extremes of exterior conditions. Thus, they account for the fact that in summer the exterior conditions add heat to the coach and that in winter the exterior conditions remove heat from the coach. Therefore, in summer the coach interior is typically warmer than in winter. Thus, an acceptable range of interior temperature is the extreme from both seasons at 68–76 °F.

The comfort zone temperature variation given in the PRIIA document does not specify a location at which the temperature is to be measured. Since the actual temperature variation allowed by stacking up the ranges listed above can be greater than the 4 °F temperature design range of each of the seasonal conditions, the researchers interpret the specification to mean the average air temperature within the passenger car should remain within the 68–76 °F range.

2.2. Field Tests on Passenger Coaches for Thermal Model Validation

Phase I modeling showed that the maximum time of HVAC shutoff under peak traction demands did not exceed 10 minutes [2] [3]. To validate the train operation and simulation analysis results of Phase I, tests were carried out on a bi-level and a single level commuter passenger coach built in 2001. This car was built prior to the development of the PRIIA specifications. The comfort limits in PRIIA are monitored and enforced through the HVAC control system and do not necessarily drive the heat transfer behavior of the car which is a function of design, i.e., construction materials and insulation. This testing had two objectives: (1) to measure the time durations for the coach interior temperature to exceed the PRIIA comfort range after shutting off the HVAC, once the acceptable temperature had been achieved; and (2) to collect temperature rise time history data to validate the thermal model developed in Phase I.

2.3. Bi-level Coach Temperature Testing

Figure 2-1 and Figure 2-2 show the overall exterior and interior view, respectively, of the bi-level passenger coach selected for temperature testing. As shown in Figure 2-3, between the lower and upper levels of the bi-level coach a total of six thermocouples were installed, and the thermocouples were placed approximately 3 ft. above the floor. The ambient conditions and the corresponding solar radiation values of the tests conducted are shown in Appendix A.

Figure 2-1. Bi-level passenger coach selected for temperature testing

Figure 2-2. Instrumentation of the bi-level passenger coach

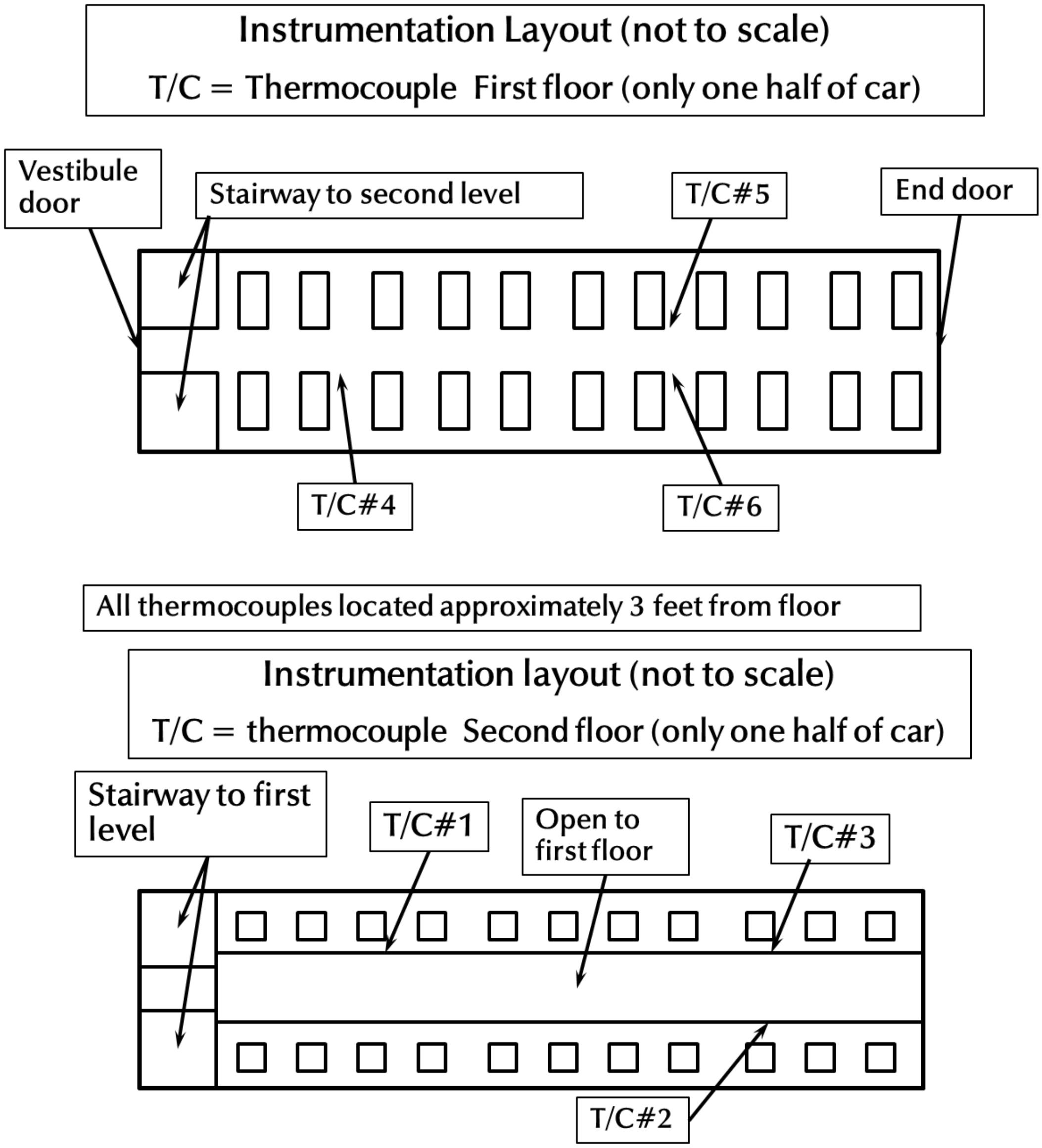

Figure 2-3. Thermocouple locations on the first and second floors of the bi-level passenger coach

Generally, passenger coaches are not highly insulated and significant wall area consists of window glazing which are poor insulators. These two factors tend to result in relatively rapid rise or drop in the interior temperature of a passenger coach following an HVAC or heating system shutoff, respectively. To capture this quick rise in temperature post HVAC shutoff, specialized thermocouples were used. In these thermocouples, a portion of the exposed wires is bent just before the junction, see Figure 2-4. This improves the heat transfer rate and thus the measured air temperature stabilizes more rapidly than with standard thermocouples.

Figure 2-4. Thermocouple used for temperature measurement

As measured, temperatures from the six thermocouples on the bi-level coach after the air conditioning (AC) shutoff are shown in Figure 2-5. At the time of shutoff, the six thermocouples show a range of 71 °F–75.3 °F indicating that during the period when HVAC is running the temperature within the interior of the coach is not uniform, though it is within the PRIIA bounds. Note that one of the thermocouples on the upper level (Upper Location 1) is 75.3 °F and almost at the upper bound of the PRIIA limits, i.e., 76 °F. The interior temperature begins to rise quickly after the AC shutoff and all thermocouples exceed the upper bound of PRIIA within 1.5 minutes. The rise in temperature slows with time but within 9 minutes, all thermocouples show temperatures well above the comfort limit.

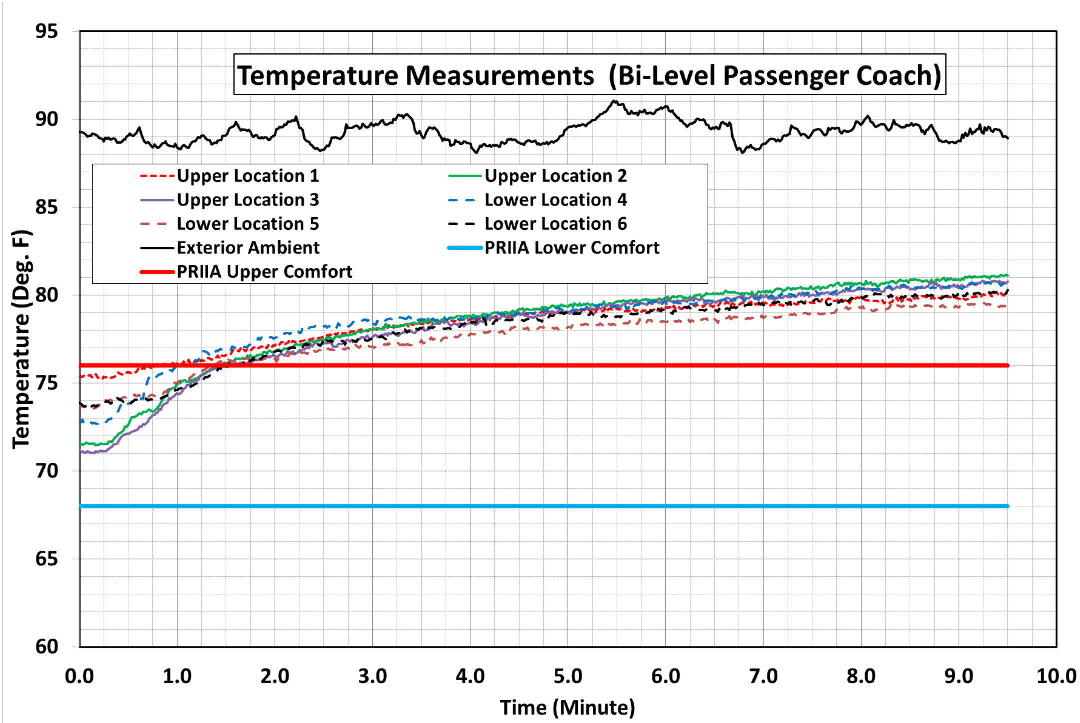

Figure 2-5. Temperature rise time history measured on bi-level coach—as recorded

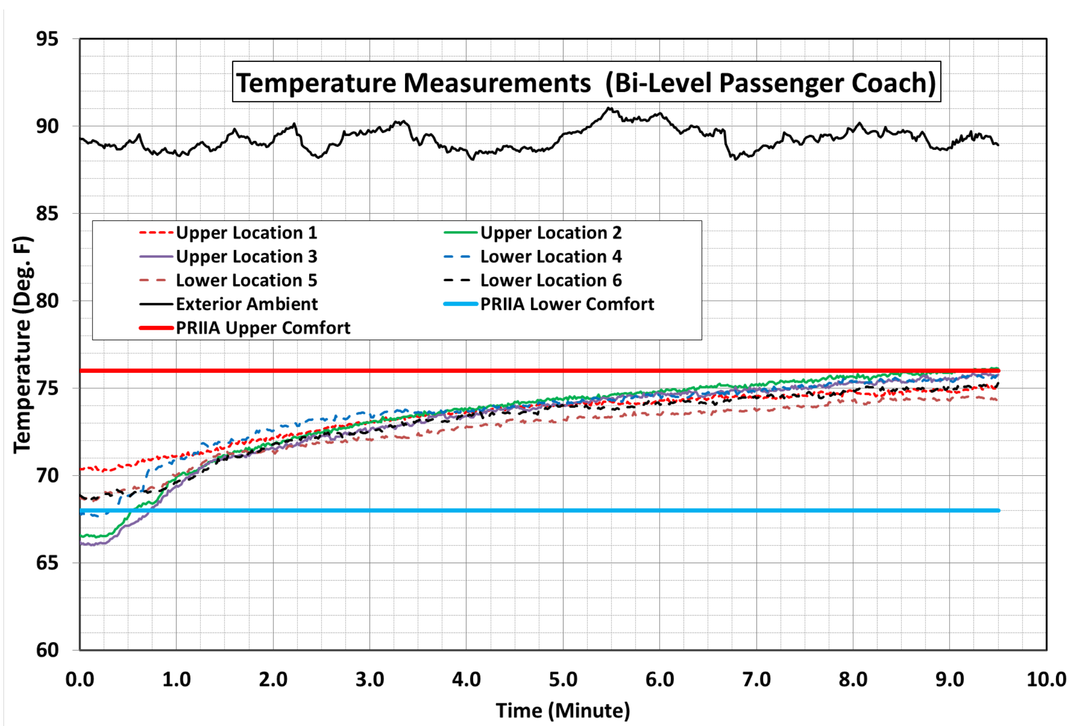

Figure 2-6. Temperature rise time history on bi-level coach—offset to lower PRIIA bound

To investigate how the duration of temperature increase would be affected if the coach had been cooled towards the lower PRIIA limit, the measured data was offset by 5 °F down—a temperature such that the thermocouple with the highest temperature (Upper Location 1 reading 75.3 °F) would record a temperature of 70.3 °F. This shifted temperature data history is shown in Figure 2-6. It is seen in this figure that, when cooled to the lower end of the bound, the coach would take almost 9.5 minutes to reach the upper PRIIA limit of 76 °F.

2.4. Single Level Coach Temperature Testing

Tests were also conducted on a single level coach. Figure 2-7 and Figure 2-8 show the overall exterior and interior view, respectively, of the single level passenger coach used for temperature testing. As shown in Figure 2-9, for the single level coach, a total of four thermocouples were installed and were placed approximately 3 ft. above the floor.

Figure 2-7. Single level passenger coach selected for temperature testing

Figure 2-8. Instrumentation of the single level passenger coach

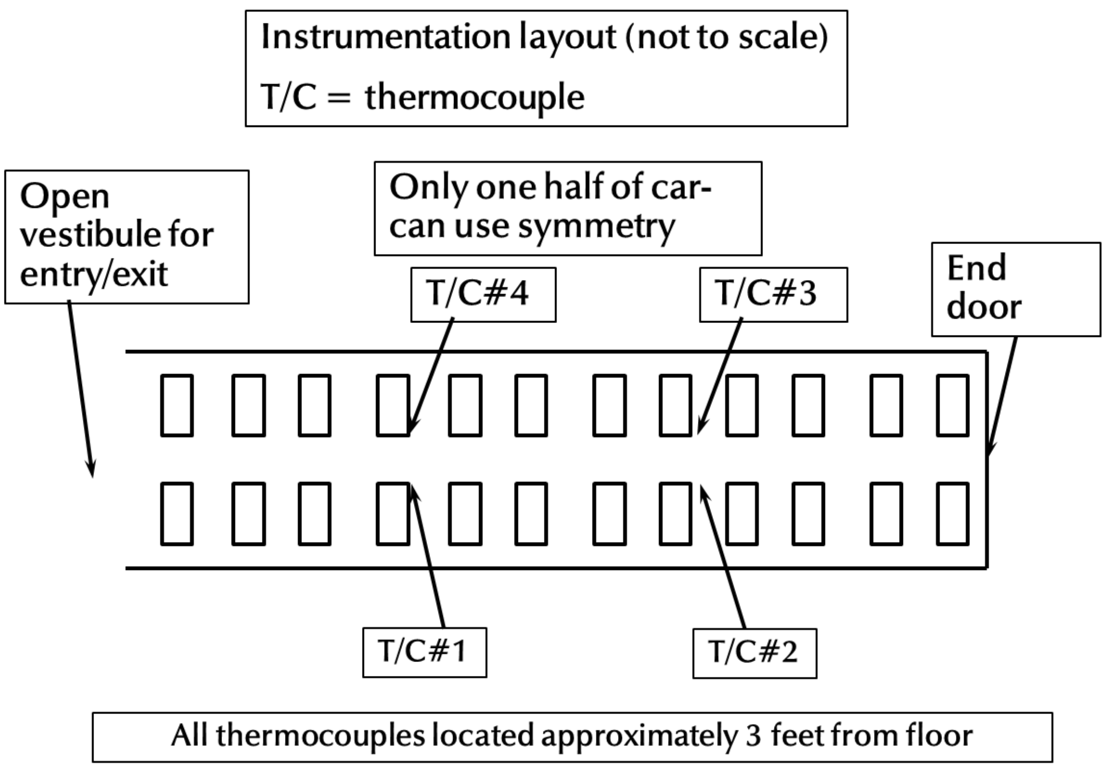

Figure 2-9. Thermocouple locations in the single level passenger coach

The recorded temperatures from the four thermocouples are shown in Figure 2-10. At the time of AC shutoff, the four thermocouples in locations 1 through 4 show interior temperatures of 72, 73.9, 72.9, and 73.1 °F, respectively. It is visible that the interior temperature begins to increase as the HVAC system shuts down. Ambient exterior temperature throughout the testing period stays mostly over 92 °F degrees and there is solar radiation flux entering through the right-side windows exposed to the sun.

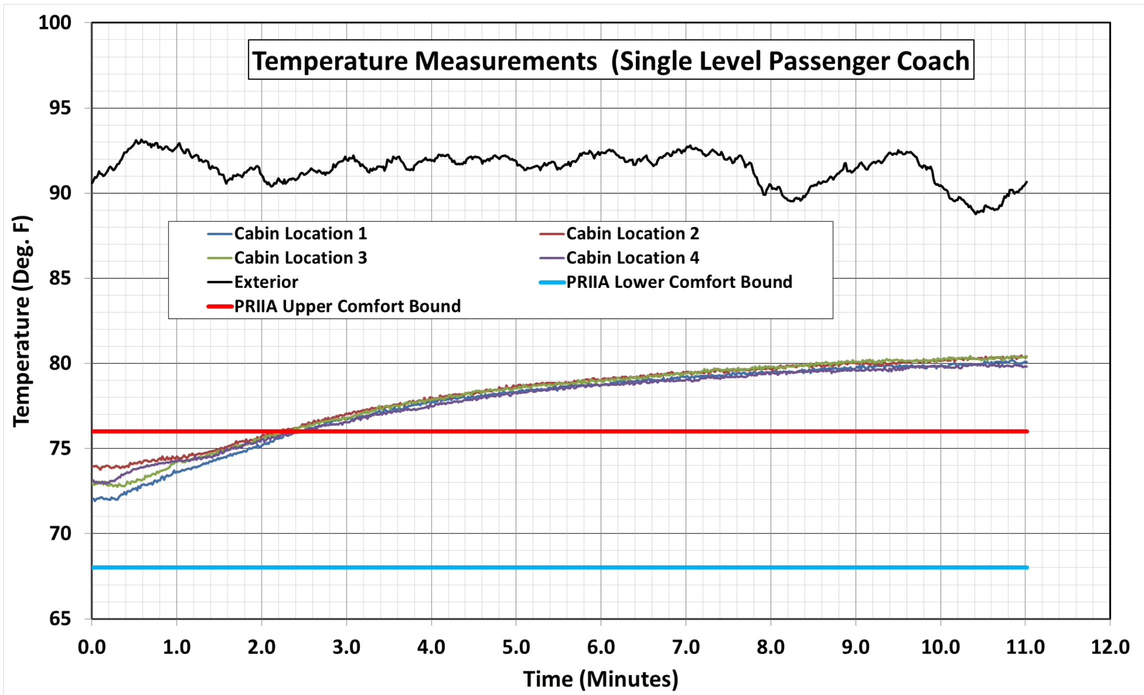

Figure 2-10. Temperature rise time history measured on single level coach—as recorded

In the early few minutes of the post shutoff period, the temperature rises faster than during the later period. This is the result of the temperature difference between the car interior and the coach walls and floor. Within the first 2.5 minutes of the recorded period, inside temperatures on all four thermocouples reach the upper PRIIA comfort limit of 76 °F. The rate of rise slows down with time as the difference between the exterior and interior reduces. At the end of the recording period of 11 minutes, the four thermocouples show stabilized temperatures well above the PRIIA limit of 76.4 °F.

Similar to the bi-level coach case, the measured data was offset by 3 °F down, such that the average of the four thermocouples, i.e., 70 °F temperature, will be near the lower PRIIA limit of 68 °F. This shifted temperature data history is shown in Figure 2-11. It is seen in this figure that when cooled to the lower end of the bound, the coach would take about 6.5 minutes to reach the upper PRIIA limit of 76 °F.

The duration under which a coach would reach the bounds of PRIIA limits is highly dependent on the outside ambient conditions and the temperature inside the coach when load shedding requires turning off the HVAC system.

The variations in the time duration between the bi-level and single level coach temperature rise leads to the observation that implementing a load-shedding strategy would require a continuous coach temperature monitoring system and communication system to alert the locomotive engineer in maintaining the PRIIA comfort temperature requirements.

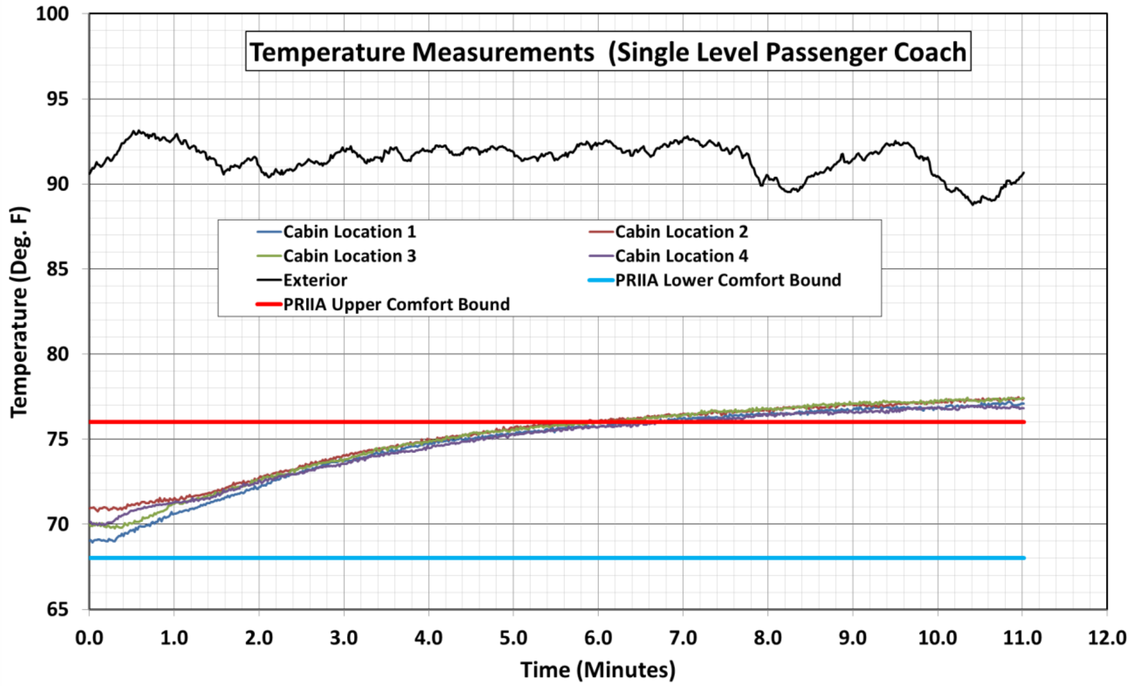

Figure 2-11. Temperature rise time history measured on single level coach—offset to lower PRIIA bound

3. Thermal Model Validation

In Phase I, a thermal model of a typical passenger coach was developed to simulate heating and cooling of the interior under load shedding conditions when the HVAC is shut off [2]. Such a model allows for investigation of train operations under varying climate conditions and to relate that to load-shedding strategies to suit the seasonal temperature effects. As seen from the temperature testing discussed in Section 2, the duration of the HVAC shutoff is highly dependent on the ambient temperature encountered by the trains in need of load shedding.

3.1. Computational Fluid Dynamics Model

For comparison with the test results, a geometric model of the interior of a long distance, single level passenger coach was considered for CFD analysis. Only one-half of the car was modeled, since the car is symmetrical about the central transverse plane.

Altair Hypermesh meshing software was used to develop the finite element mesh model. The details of the mesh model are shown in Figure 3-1 to Figure 3-4. The seats were modeled using a representative model, to account for the obstructions to the air flow.

There were only one or two testing engineers in the car during the test. To simulate the testing conditions, passengers were not considered in this analysis. The air volume of this model was used for the flow and thermal analysis using the Abaqus CFD solver program.

The passenger car was simulated in the heating condition (i.e., in the summer, when HVAC is turned off, and the car heats up) to determine the time required for the average interior temperature to rise beyond the levels of comfort specification.

Computation of heat transfer through the solid layers is explained below.

Each wall is considered individually for computing the heat transfer. All the walls/structures considered for heat transfer calculation are listed below:

1. Side wall facing the sun
2. Side wall in the shade
3. Roof, facing the sun
4. Back wall, facing the sun
5. Floor, in the shade
6. Windows facing the sun

Initial interior air temperature of 70 °F and a constant exterior environment temperature of 91.5 °F were assumed based on test data. For each of the walls/structures, a simple heat balance equation was used to calculate the outer wall temperature and the corresponding heat transfer into the car through the wall/structure.

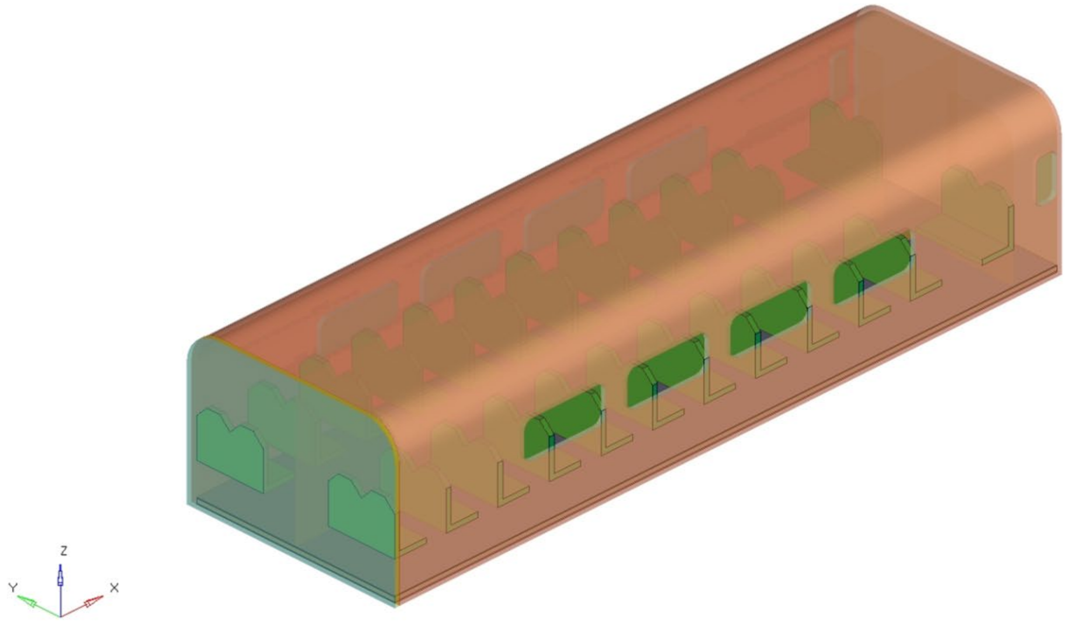

Figure 3-1. Finite element model (half coach) including walls, floor, roof, seats, and windows (260,956 nodes, 547,959 elements)

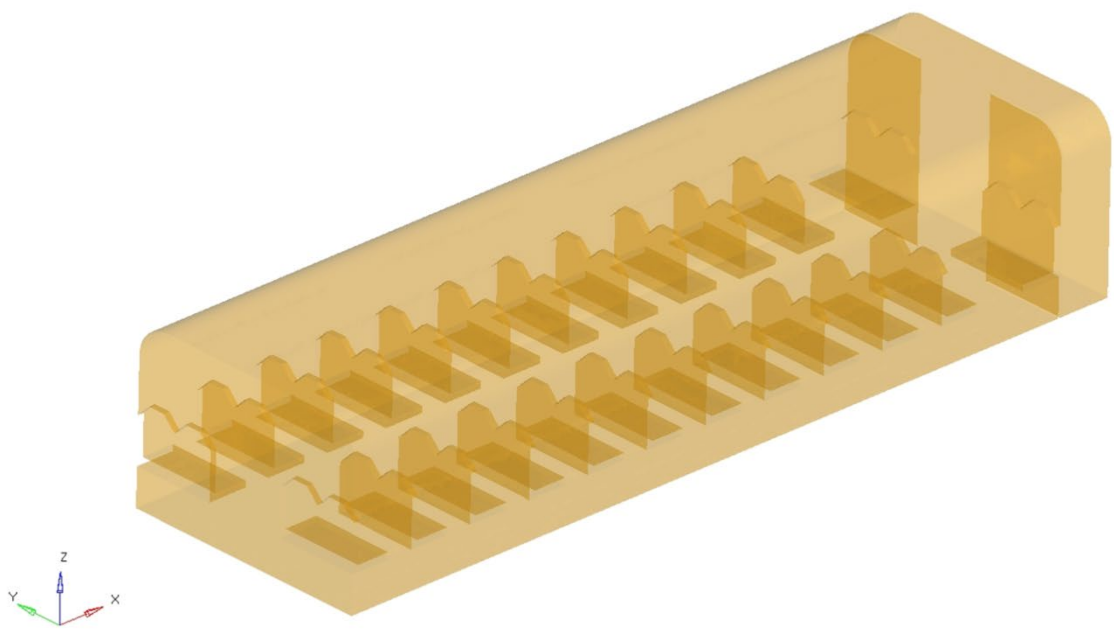

Figure 3-2. Finite element model for air volume only (233,338 nodes, 1,172,792 elements) seats shown for location

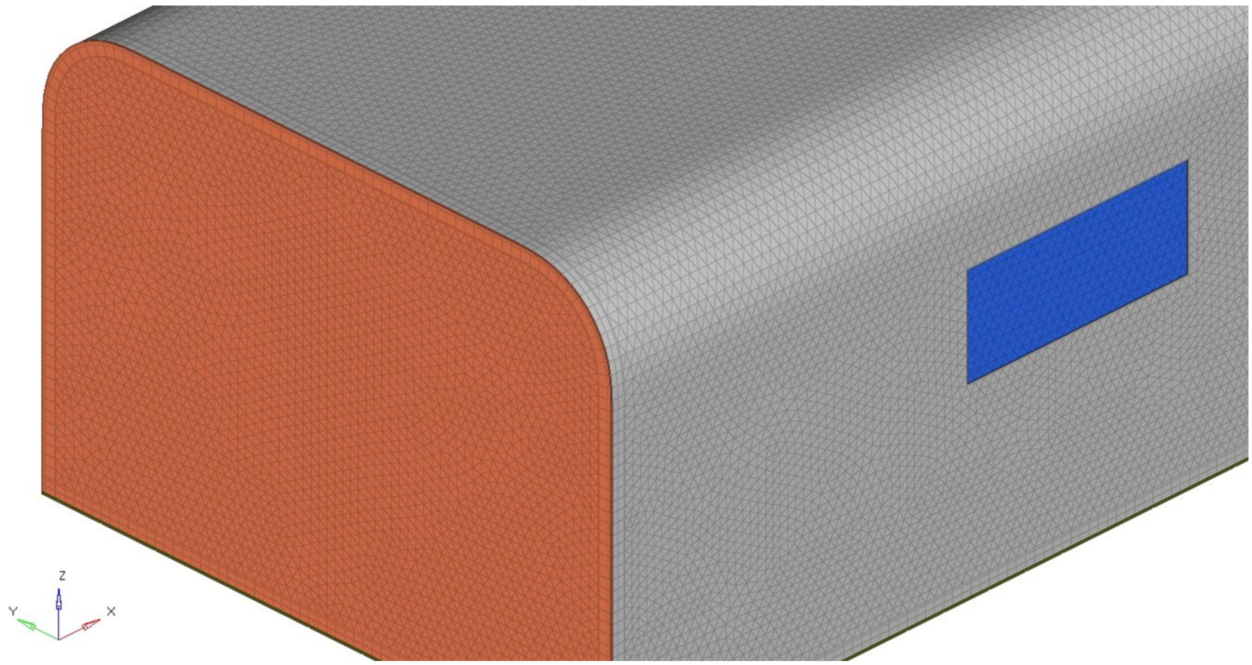

Figure 3-3. Finite element mesh details for solid material

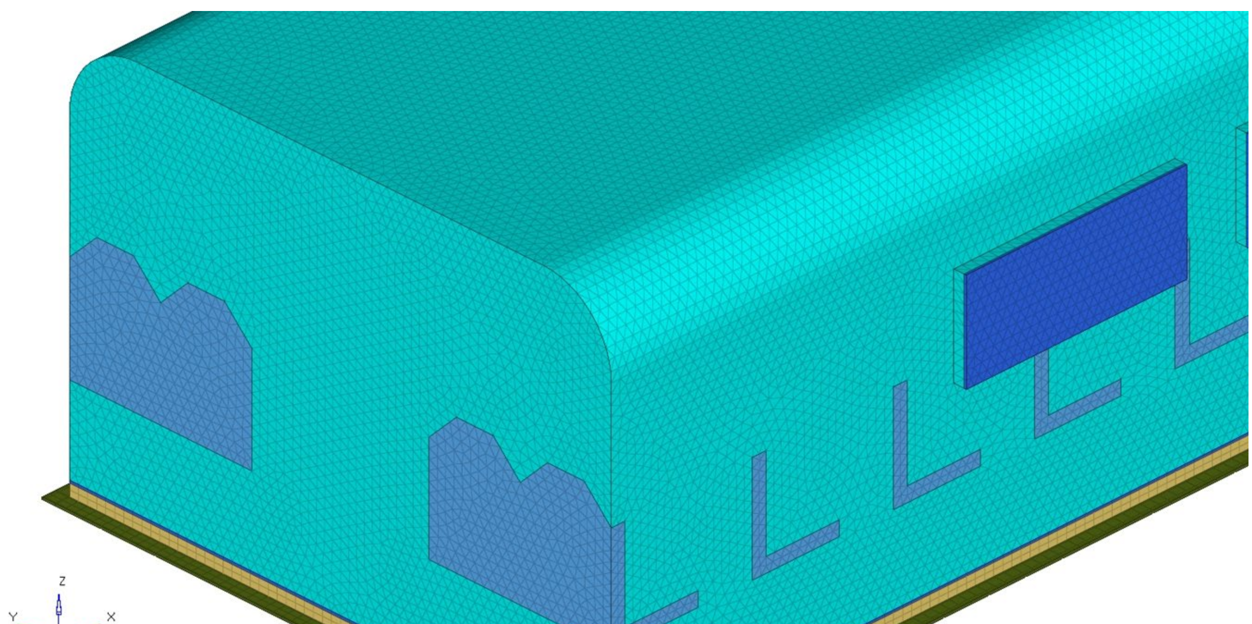

Figure 3-4. Finite element mesh details for air volume

The structures facing the sun have the following modes of heat transfer:

(a) Solar radiation into the outer wall

(b) Radiation of outer wall into the surroundings (ambient air)

(c) Convection at outer wall into the surroundings

(d) Conduction into the car

The structures in the shade have the following modes of heat transfer:

(a) Radiation of outer wall into the environment

(b) Convection at outer wall into the surroundings (ambient air)

(c) Conduction into the car

The thermal model material properties are included in Appendix B. Computational method details of the heat transfer calculation for all the structure components are shown in Appendix C.

The heat transfer is calculated once a minute from the one-dimensional model, to account for the reduced rate of heat transfer with the increase in the interior temperature. This calculated heat transfer through conduction into the car, after accounting for the thermal mass of seats and other structures, is given as the heat flux input to the CFD model of air. This heat flux was uniformly distributed across all the exterior nodes of air volume. CFD simulation was carried out using Abaqus CFD software. Interior air temperature states are shown in Figure 3-5 through Figure 3-10. Air temperature after 11 minutes of simulation was 78 °F, a rise of 8 °F from the starting point of 70 °F, which is in agreement with the test temperature of 77 °F at the end of 11 minutes.

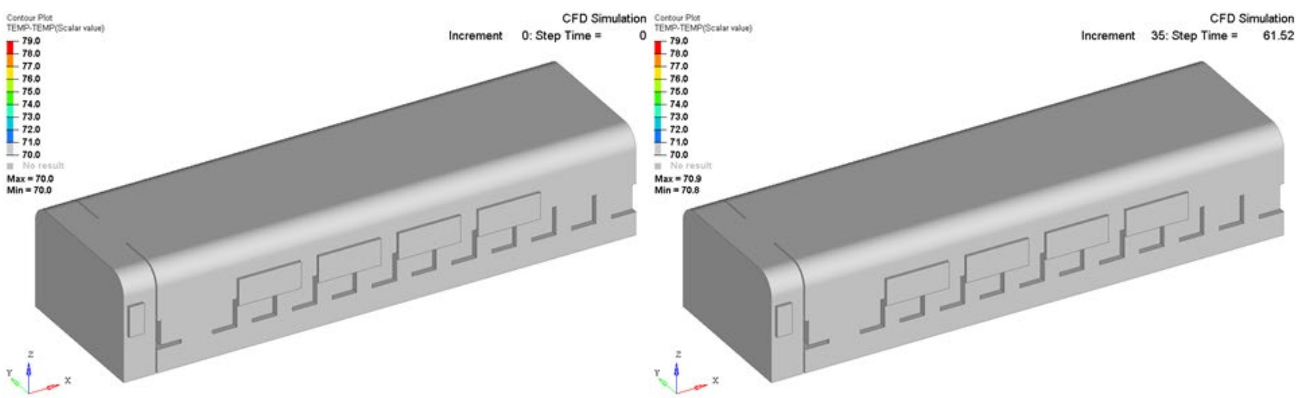

Figure 3-5. Air volume CFD model predicted temperature in the interior at the start (left, 70.0 °F) and after 1 minute (right, 70.9 °F)

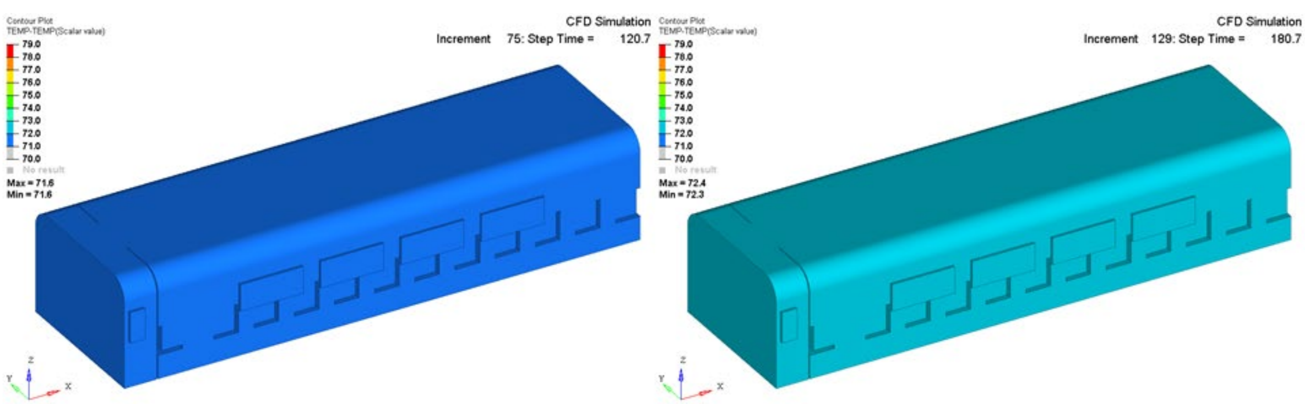

Figure 3-6. Air volume CFD model predicted temperature in the interior at the end of 2 minutes (left, 71.5 °F) and 3 minutes (right, 72.4 °F)

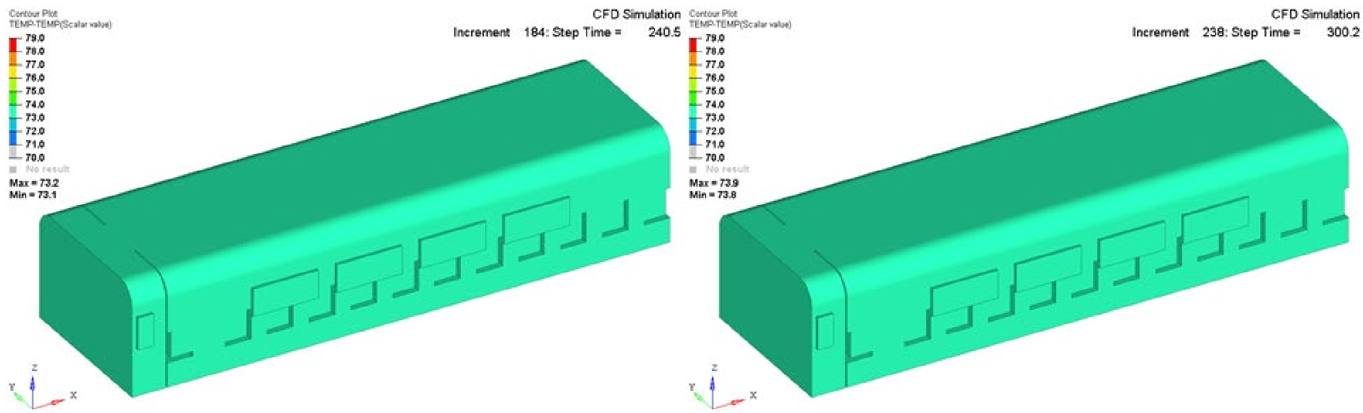

Figure 3-7. Air volume CFD model predicted temperature in the interior at the end of 4 minutes (left, 73.2 °F) and 5 minutes (right, 73.9 °F)

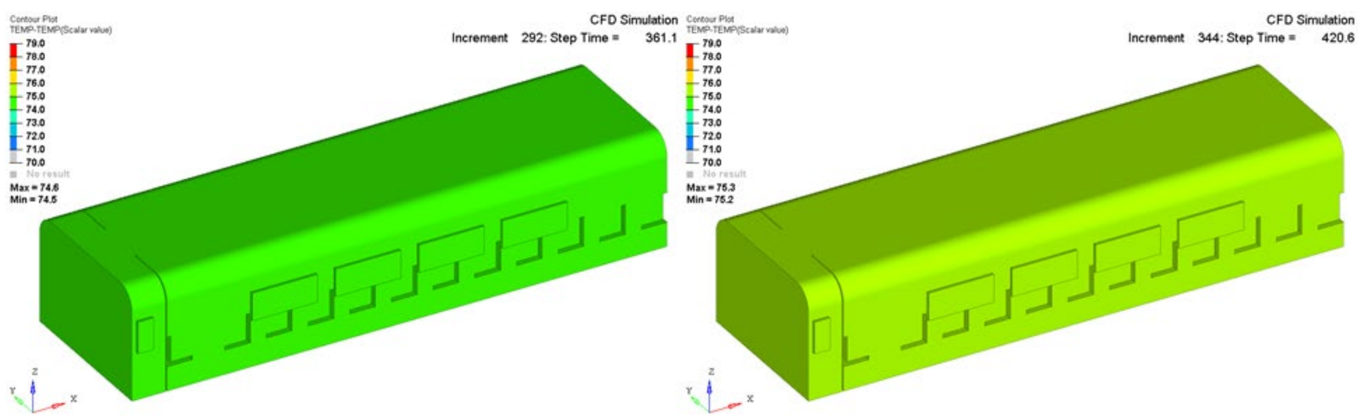

Figure 3-8. Air volume CFD model predicted temperature in the interior at the end of 6 minutes (left, 74.6 °F) and 7 minutes (right, 77.9 °F)

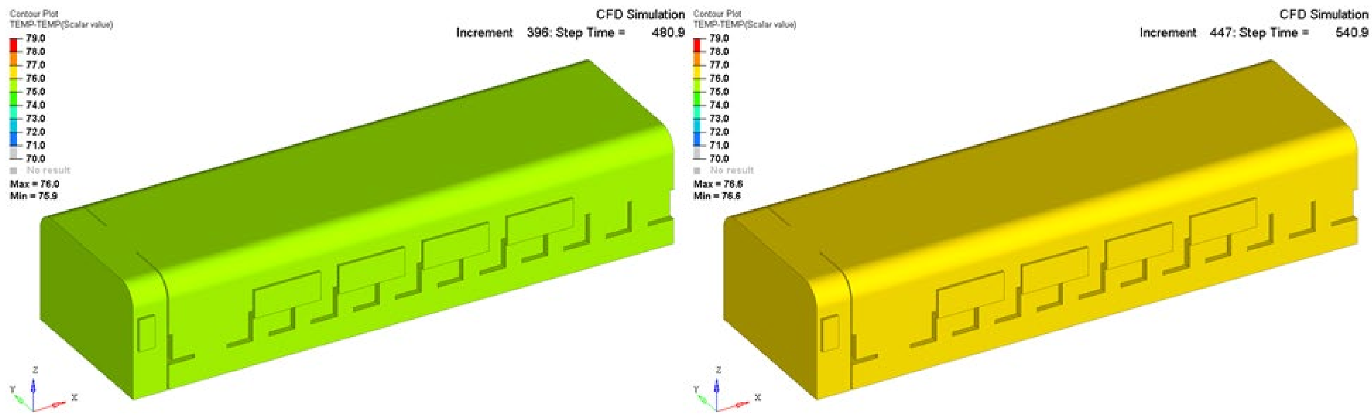

Figure 3-9. Air volume CFD model predicted temperature in the interior at the end of 8 minutes (left, 76 °F) and 9 minutes (right, 76.6 °F)

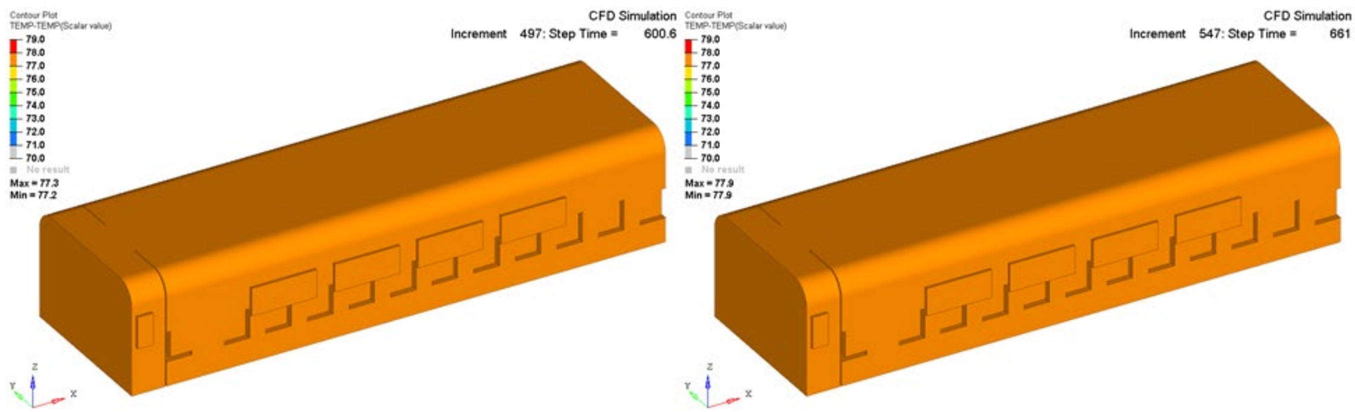

Figure 3-10. Air volume CFD model predicted temperature in the interior at the end of 10 minutes (left, 77.3 °F) and 11 minutes (right, 77.9 °F)

4. Load Shedding Monitoring System Concept

This section describes the communication hardware including the PLC and the selected protocol based on widespread practices in industrial applications.

4.1. Programmable Logic Controller (PLC) Modbus RTU

Modbus RTU is an open serial protocol derived from the Master/Slave architecture originally developed by Modicon. It is a widely accepted serial level protocol due to its ease of use and reliability.

The proposed architecture discussed in the following section uses Modbus RTU communication between vehicles. The locomotive would be equipped with a 750-881 (or similar) programmable fieldbus coupler, the required discrete input modules to sense the throttle position, and an RS-485 communications module. The locomotive would also be equipped with a Human-Machine Interface (HMI) that would interface with the programmable coupler via Ethernet. Each of the passenger coaches would be outfitted with identical systems consisting of a 750-881(or similar) programmable coupler, a relay output module to control the HVAC system, a Resistance Temperature Detector (RTD) temperature module, and two RS-485 communication modules.

The RS-485 module on the locomotive would be configured as Modbus station number 1. This module would be connected to a similar module on the next car that would be configured as Modbus station number 2. This first car would have a second module configured as Modbus station number 1 on a separate Modbus network which would be connected to the communication module on the next car which would be configured as Modbus station number 2. Thus, the train would have multiple independent Modbus networks, each have two stations with IDs 1 and 2. Each programmable coupler would attempt to communicate with a Modbus station number 2 using its module configured as station number 1. Data could then be propagated through the train station-by-station.

Because each Modbus network has only two stations, the station IDs can be static and terminating resistors can be permanently placed, satisfying the requirement of not requiring technical intervention to assemble the consist. However more information is required to determine if this would be a workable solution form a programming standpoint.

5. Network Architecture

The proposed system Modbus RTU network functionality as relating to the locomotive and coaches in the train is described in this section. The proposed network architecture uses Modbus RTU to transmit messages throughout the train consist. Figure 5-1 shows a network diagram for a three-car train, with the proposed hardware.

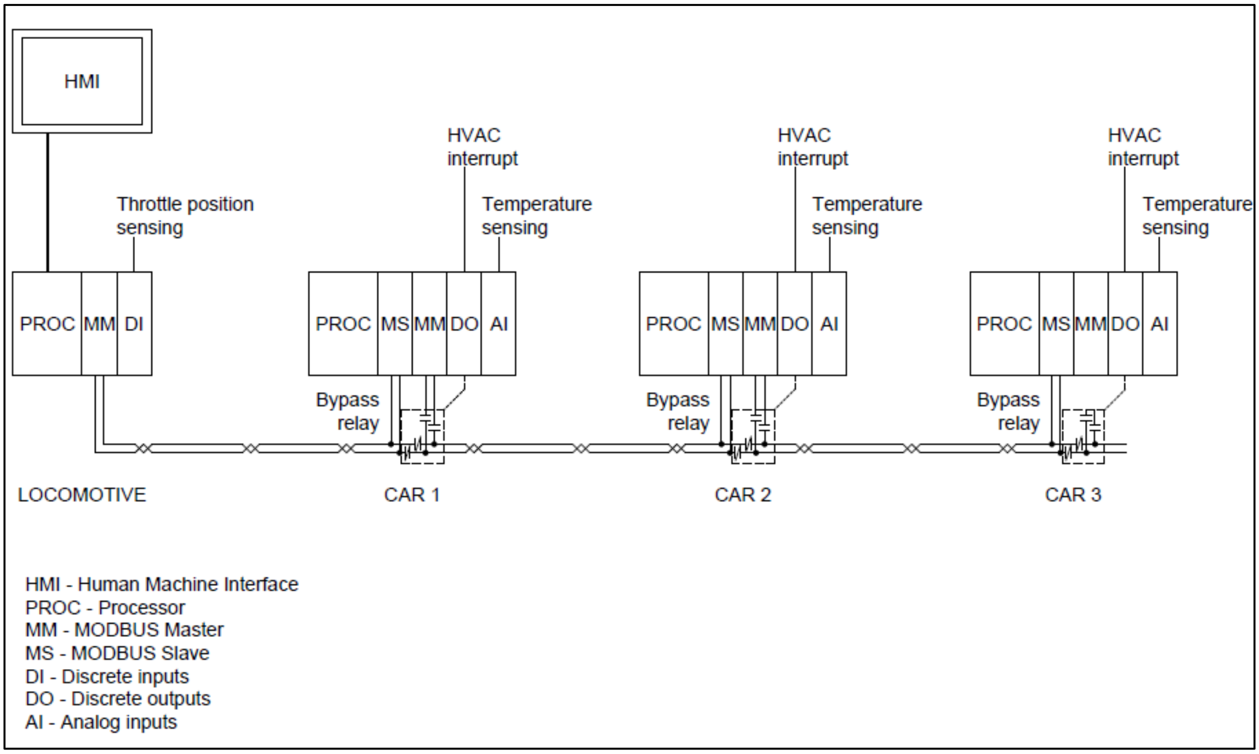

Figure 5-1. Modbus RTU network diagram

Each locomotive will have a single communication module for communicating with the first car. Each passenger car will have two Modbus RTU modules: one module communicates directly with the adjacent car towards the lead or locomotive, and the other module communicates directly with the adjacent car towards the rear. These connections continue for all vehicles in a train. Thus, the train network consists of a daisy-chain of multiple peer-to-peer networks between adjacent cars. Communication and control software will be written to accommodate variability in the relative car position and orientation in the train.

6. Load Shedding Hardware

The load-shedding system will require monitoring and communication control hardware. The HMI for this purpose, located in the locomotive cab, is discussed in this section.

6.1. Human Machine Interface

An HMI will be integrated into the system, located inside each locomotive cab. This interface has not been completely identified yet. However, the intent of this load-shedding system is to operate automatically, so the HMI will likely be a display with minimal controls. The display will only provide information to the operating engineer. This information will include individual car temperature, load-shedding status, and diagnostic information. A main interlock power control will be available to the operating engineer, if it is desired to shut down the train-wide load-shedding system.

6.2. Passenger Car Hardware

Every type of passenger car in this concept will be equipped with the load shedding equipment. Each car will have a PLC consisting of various individual modules. Each PLC will have a main processor node, a relay output module, an RTD input module, network communication modules, and any additional operating modules necessary for the specific PLC.

The main processor module will allow for in-system troubleshooting and diagnostics. It will have an Ethernet port or a serial port for connecting to a laptop.

The relay output module would be used for interfacing with the onboard HVAC system. There are a few options for the HVAC interface, as described in Section 6.3.

The RTD input module would be used for connecting to an RTD type temperature sensor. It is necessary for the PLCs to monitor and record interior car temperatures to determine whether load shedding should end.

The network architecture proposed, as described earlier, uses Modbus for PLCs to transmit messages throughout the consist. Each passenger car PLC will have two Modbus RTU modules: one module communicates directly with the adjacent car towards the lead or locomotive, and the other module communicates directly with the adjacent car towards the rear. The modules are wired for peer-to-peer communication using shielded twisted-pair cable. Appropriate termination hardware will be implemented to minimize transmission line losses.

6.3. HVAC Interface

Depending on the HVAC system installed on each car, there are several possible solutions for interfacing the PLC with the car's HVAC system.

The prevailing path is to have a generic relay output module in the PLC. The PLC logic controls the relay contacts, which controls power to the HVAC system. The relays would be normally closed for appropriate failsafe. This concept is simple, but it introduces issues with cycling HVAC power.

Another idea for an interface between the control system and the HVAC system is to interface with an existing, or implement a new, control network. It is believed that many HVAC systems may have diagnostic HMI networks operating over a serial type control network, such as

RS-232. There are serial communication modules that can be incorporated into the PLCs at each car. The hope is that these modules can be programmed to communicate with the HVAC system to control its output. This would be a preferred method if the capability exists.

6.4. Network Hardware

The cabling and interior wiring for both the locomotives and passenger cars must have the two-way communications available, which requires at least two wires in the cable running the length of the train. Physically speaking, two wires will only go from the PLC to the front connector and two wires will go from the PLC to the rear connector.

Presently, the communications trainline has no spares in the 27-pin cable as shown in the PRIIA document [1]. However, pins 3-4, 9-10, and 24-25 are each reserved for digital trainline/passenger information. It should be possible to design a communication system that can utilize one of these wire pairs to send the load shedding data without disturbing other signals being passed through. All passenger coaches and passenger locomotives must be configured to utilize this communications cabling to implement load shedding.

In the case of passenger cars used for transporting cargo, such as baggage cars, PLCs will not be installed. Therefore, it is necessary for communication to bypass through these cars to adjacent cars. Signal integrity must be maintained throughout the consist, so that any single car does not introduce unacceptable impedance on the network.

7. Load Shedding Software

Load shedding will follow the general system state diagram shown in Figure 7-1. This state diagram is meant to serve as a general guideline for developing the software for the PLCs on the locomotive and passenger cars. Actual programming will depend on optimal and efficient coding practices.

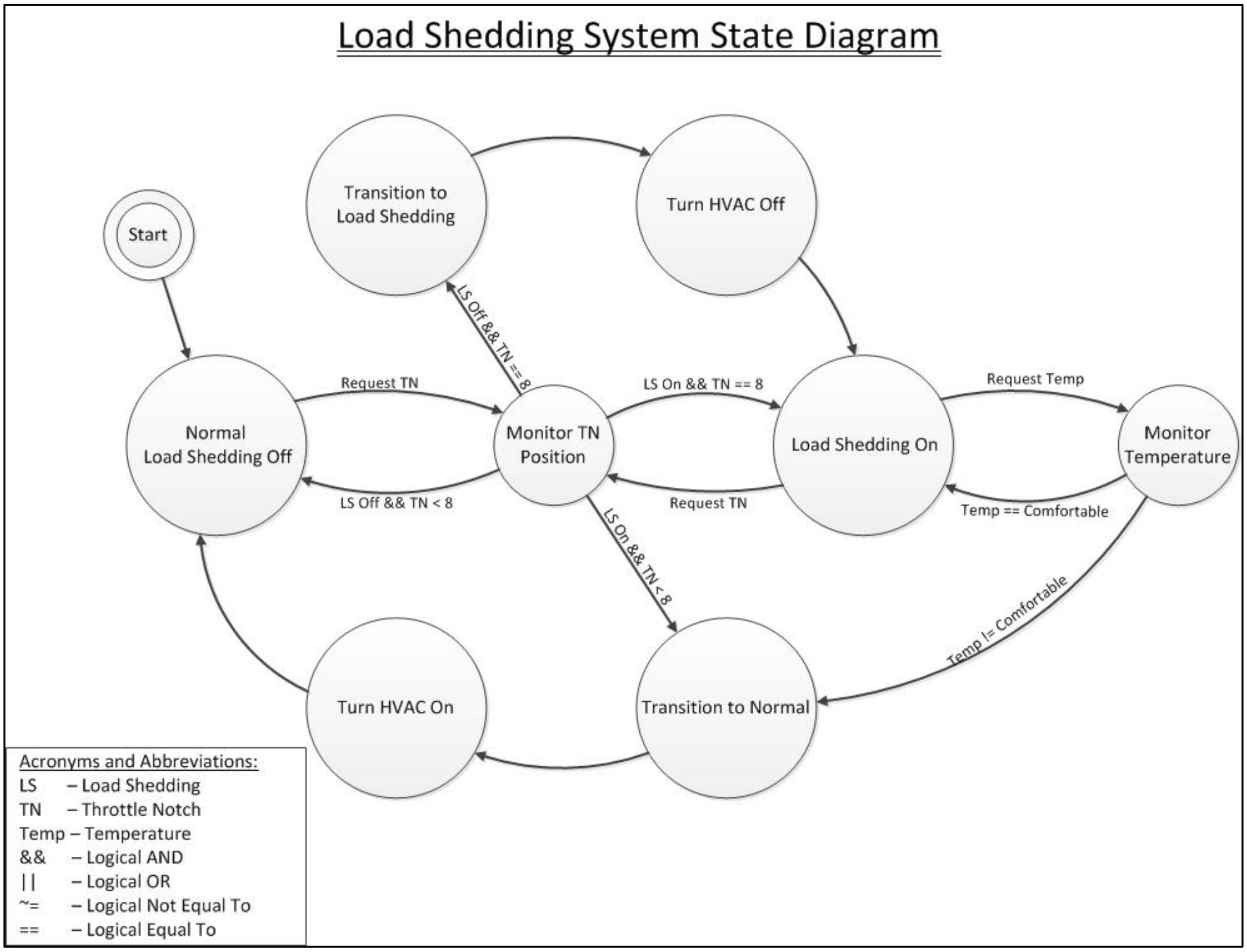

Figure 7-1. Load shedding state diagram

7.1. Communication Protocol

The network uses Modbus RTU protocol for transmitting data between nodes. Modbus is a serial communication protocol, used extensively in industrial automation.

Table 1 lists all the defined variables used in the system. Each variable is allocated a certain data size for current necessity and future compatibility. Variable ranges are also defined within the limits of load shedding and practical passenger applications.

Table 1. Variable explanation

Variable Name	Description	Bits	Range	Remarks
CAR_COUNT	Number of cars in consist	16	[0, 32]	Abbreviated as *N*
LIMIT1	Temperature limit-exceeded Word for cars 1–16	16	[0, 0xFFFF]	Bit0 = Car 1
LIMIT2	Temperature limit-exceeded Word for cars 17–32	16	[0, 0xFFFF]	Bit0 = Car 17
WARN1	Temperature warn-exceeded Word for cars 1–16	16	[0, 0xFFFF]	Bit0 = Car 1
WARN2	Temperature warn -exceeded Word for cars 17–32	16	[0, 0xFFFF]	Bit0 = Car 17
MY_TEMP	Conceptual array for storing every car's temperature	16**N*	[-32768, 32767] (per element)	
MY_STATUS	Shifted bit for temperature status at this car	1	0 = inside limit 1 = outside limit	Bit0 = Car1 OR Car 17
COMMAND	Locomotive command for controlling load-shedding states	16	See Table 2	Extra bits available for future use
LIMIT_HIGH	Lower Temperature Limit	16	[-32768, 32767]	User configurable
LIMIT_LOW	Upper Temperature Limit	16	[-32768, 32767]	User configurable
WARN_HIGH	Lower Temperature Warning Threshold	16	[-32768, 32767]	User configurable
WARN_LOW	Upper Temperature Warning Threshold	16	[-32768, 32767]	User configurable

The number of cars will be identified by an initial query-and-response procedure. The locomotive transmits a query message to the first car in the train, and waits for a response. Once the first car replies to the locomotive, that car transmits a similar message to the next car in the train and waits for a response. The CAR_COUNT variable is updated every transaction. This procedure continues until the last car does not receive a response.

The limit and warning thresholds are LIMIT_HIGH, LIMIT_LOW, WARN_HIGH, and WARN_LOW. These thresholds can be configured by an authorized maintenance person. The values represent degrees in Fahrenheit times 10, with 1 decimal place (e.g., a value of 1,000 means 100.0 °F).

The limit and warn variables are LIMIT1, LIMIT2, WARN1, and WARN2. These variables indicate the temperature status of all cars in the train. The car's status is represented in a single bit shifted by the car's position in the train. The Least Significant Bit (LSB) represents car 1, for

LIMIT1 and WARN1, and the Most Significant Bit (MSB) for car 17 for LIMIT2 and WARN2. A bit value of one indicates the temperature is outside the comfort range, as specified by the threshold constants.

The COMMAND variable will be a 16-bit type value used by the locomotive for giving instructions to cars. The variable has been given extra bits for future compatibility. Table 2 lists the possible values for each bit in the COMMAND variable with descriptions.

Table 2. COMMAND variable bit-fields

Bit	Action	Description
0	Consist stable	0 = Train not built yet or issue present 1 = Train built and stable
1	Activate load-shedding	0 = Deactivate load-shed 1 = Activate load-shed
3–15	Reserved for future use	Set to 0

All messages in the network will follow the generic message structure in compliance with Modbus RTU. Each Modbus data field has 40 register offsets. Table 3 lists the contents for each register for all Master Read (Slave Write) messages, for locomotive and cars. Table 4 lists the contents for each register for all Master Write (Slave Read) messages, for locomotive and cars.

Table 3. Modbus message data field table for master reads

Modbus Register Offset	Locomotive (Master Only)	Car, n	
		Slave Module	Master Module
0	CAR_COUNT	CAR_COUNT	CAR_COUNT
1	LIMIT1	LIMIT1 | MY_STATUS	LIMIT1
2	LIMIT2	LIMIT2 | MY_STATUS	LIMIT2
3	WARN1	WARN1 | MY_STATUS	WARN1
4	WARN2	WARN2 | MY_STATUS	WARN2
5–37	MY_TEMP [1:N]	MY_TEMP [n:N]	MY_TEMP [n-1:N]
38–40	Reserved for future use	Reserved for future use	Reserved for future use

Table 4. Modbus message data field table for master writes

Modbus Register Offset	Locomotive (Master Only)	Car, n	
		Slave Module	**Master Module**
0	1	MY_ID	MY_ID + 1
1	COMMAND	COMMAND	COMMAND
2	LIMIT_HIGH	LIMIT_HIGH	LIMIT_HIGH
3	LIMIT_LOW	LIMIT_LOW	LIMIT_LOW
4	WARN2	WARN2	MY_STATUS	WARN2
5	WARN_HIGH	WARN_HIGH	WARN_HIGH
6–40	Reserved for future use	Reserved for future use	Reserved for future use

8. Proof-of-Concept Testbed

To gain confidence in the proposed network architecture, a rudimentary proof-of-concept testbed was set up in the SA laboratory. The testbed, consisting of a 4-node network, is shown in Figure 8-1.

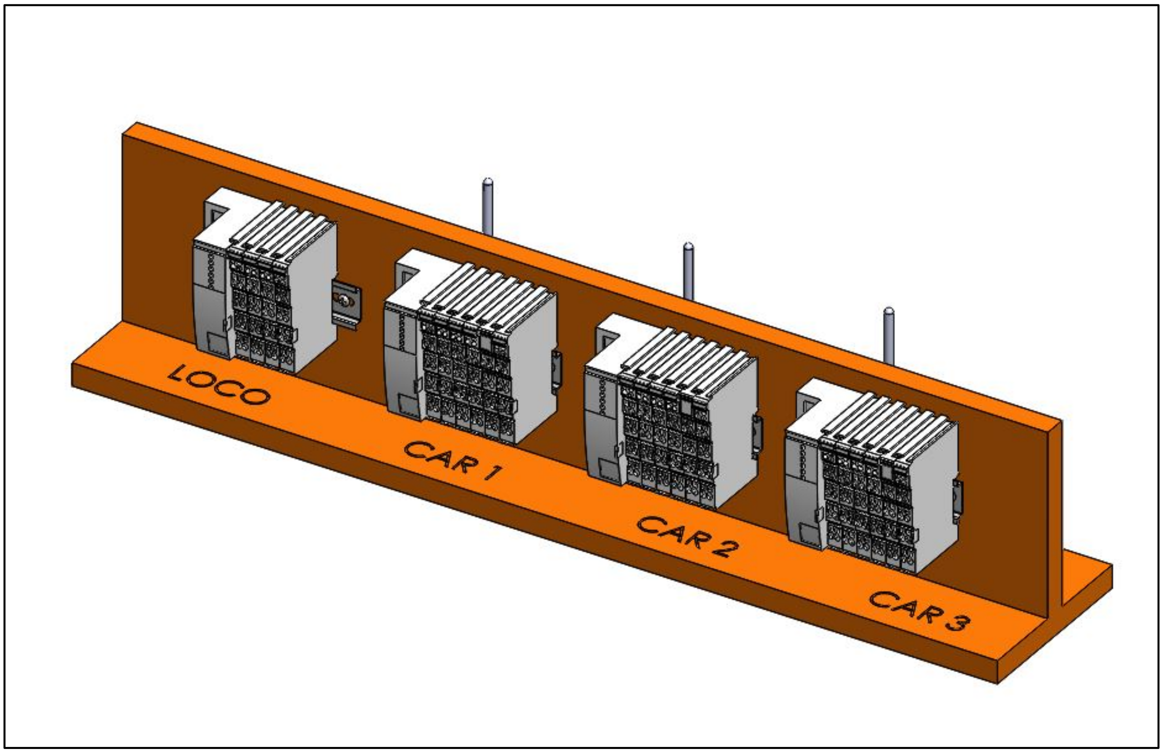

Figure 8-1. Load-shedding concept testbed

This primary reason for developing this testbed during this phase was to verify that the communication modules can dynamically and automatically configure themselves, regardless of position and orientation. This is an essential requirement for this system, so that load-shedding system initialization does not impede normal train building operations. Additional load-shedding functionality was also developed and tested using the testbed. Using this testbed, SA was able to realize the software concepts as outlined, including automatic train building.

9. Conclusion

Right-sizing a locomotive diesel engine for the various load demands on it, including traction and passenger comfort, is beneficial from multiple perspectives. The earlier effort in this area evaluated the feasibility of temporarily shedding electrical demand associated with passenger car HVAC systems during periods of peak traction needs, with the goal of right-sizing the main engine on a passenger locomotive.

Between July 31, 2017, and December 11, 2019, FRA funded SA as a part of the reported effort to conduct temperature tests on two passenger coaches. The coaches were instrumented with thermocouples to record temperature after the HVAC shutoff to investigate the time duration for the coach interior temperature to rise above the PRIIA comfort temperature limit.

Based on the simulation and measurement of temperature inside a passenger coach, a computational fluid thermodynamics model was validated for its prediction of temperature when the HVAC is turned off during load shedding. Such predictions can be used to set load shedding boundaries for the target equipment.

A finite element analysis of a typical single passenger coach was carried out for cooling conditions to determine the maximum length of time the HVAC system could be deactivated and maintain the interior air temperature within the PRIIA comfort bounds of 72–76 °F for summer. The PRIIA specifications were chosen because it is more likely that new cars and locomotives will be outfitted with load-shedding equipment.

The thermal analytical model simulations showed that it can predict temperature rise in the interior of a passenger coach when the HVAC system is shut down under load-shedding demand. The model predictions for the temperature rise and the associated time for the temperature increase were in close agreement with the field data collected in Phase II of the project.

Under the reported effort, system architecture for communication and control of the load-shedding concept was developed. The hardware components for the system were identified and procured as off-the-shelf items. Through a literature search, an appropriate communication protocol, Modbus RTU, was identified and the associated software was acquired.

A four-node network testbed was set up in the lab representing a four-vehicle train: one locomotive and three passenger coaches. The HVAC shutdown and restart of the locomotive load shedding were emulated via a laptop.

The testing verified that the communication modules can dynamically and automatically configure themselves, regardless of car position and orientation. This was an essential requirement for this system, so that load-shedding system initialization does not impede the normal train building operations.

Additional load-shedding functionality was also developed and tested using the testbed to confirm that the software functioned as laid out in concept architecture, including automatic train building.

Additional effort is recommended to implement the developed load-shedding concept on a demonstration train as a validation of the assumptions and results observed so far.

10. References

1. Passenger Rail Investment and Improvement Act, "Specification for a PRIIA Bi-Level Passenger Rail Car," Section 10.4, PRIIA Specification No. 305 001, Amtrak Specification No. 962, Revision C.1, September 20, 2012.
2. Federal Railroad Administration, "Feasibility of Load-Shedding to Improve Efficiency and Reduce Energy Consumption on Passenger Locomotives, Phase I," Technical Report No. DOT/FRA/ORD-20/29, 2020, Washington, DC: Department of Transportation.
3. Shurland, M., Andersen, D. R., Prabhakaran, A., and Singh, S. P., "Feasibility of Load-Shedding to Improve Efficiency and Reduce Energy Consumption on Passenger Locomotives," Proceedings of *the 2015 Joint Rail Conference*, March 23–26, 2015, San Jose, CA.

Appendix A.
Passenger Coach Specifications

Passenger Coaches Used for Temperature Testing	
Single-Level Length 85 ft. Width 10 ft. 6 in. Height 15 ft. 11 in. Number of Seats 96 Built 2001	
Bi-Level Length 85 ft. Width 10 ft. 6 in. Height 15 ft. 11 in. Number of Seats 156 Built 2008	

Passenger Coach Test Conditions	
Location **Date** **Time**	Northern Indiana Commuter Transportation District (NICTD) Yard, Michigan City, IN September 2, 2015 11:30 AM–1:30 PM
Temperature During Test Period Maximum, Minimum and Average	93.14 °F, 88.8 °F and 91.4 °F
Solar Radiation During Test Period Maximum Minimum Average	 830 W/m^2 748 W/m^2 800.4 W/m^2

Appendix B.
Properties of Materials Used in Analysis

Material Properties Used in the Thermal Analysis

	Density	Specific heat	Thermal conductivity	Reference: Source link
	kg/m^3	J/kg-K	W/m-K	
316 SS	8000.0	500.0	16.300	AISI Type 316 Stainless Steel, annealed sheet
Fiberglass insulation	150.0	700.0	0.040	Thermal Conductivity of selected Materials and Gases
ABS	1160.5	1475.0	0.190	
Wood–Oak	720.0	1250.0	0.160	Thermal Properties Of Building Materials
Glass	2700.0	880.0	0.800	Thermal Properties Of Building Materials
Nylon	1112.0	1600.0	0.250	Thermal Conductivity of selected Materials and Gases
Air	1.2	1005.0	0.026	Thermal Conductivity of selected Materials and Gases

Abaqus Consistent Units

	Density	Specific heat	Thermal conductivity	Dynamic Viscosity
	lbf-s^2 /in^4	in-lbf/((lbf/(in/s^2))-°F)	in-lbf/(s-in-°F)	**lbf-s/in^2**
316 SS	7.48590E-04	4.30554E+05	2.03577E+00	
Fiberglass insulation	1.40361E-05	2.41110E+05	1.24894E-02	
ABS	1.40361E-05	6.02775E+04	4.99576E-02	
Wood–Oak	1.08592E-04	1.27013E+06	2.37728E-02	
Glass	6.73731E-05	1.07638E+06	1.99830E-02	
Nylon	2.52649E-04	7.57775E+05	9.99152E-02	
Air	1.04054E-04	1.37777E+06	3.12235E-02	2.65350E-09

Appendix C.
Computation of Heat Transfer Through Solid Layers Using One-Dimensional Model

Each wall is considered individually for computing the heat transfer. All the walls / structures considered for heat transfer calculation are listed below.

1. Side wall facing the sun - side_wall_sun
2. Side wall in the shade - side_wall_shade
3. Roof, facing the sun
4. Back wall, facing the sun
5. Floor, in the shade
6. Windows facing the sun - windows_sun

Interior temperature condition of 70 °F and environment temperature of 91.5 °F was taken from the test. Simple heat balance equation was used to calculate the exterior temperature and the corresponding heat transfer into the car.

The structures facing the sun have the following modes of heat transfer:

(e) Solar radiation into the outer wall

(f) Radiation of outer wall into the surroundings (ambient air)

(g) Convection at outer wall into the surroundings

(h) <u>Conduction into the car</u>

The structures in the shade have the following modes of heat transfer:

(d) Radiation of outer wall into the environment

(e) Convection at outer wall into the surroundings (ambient air)

(f) <u>Conduction into the car</u>

The computational method and details of the heat transfer calculation for one of the walls is explained in this appendix. Sidewall in the sun is considered for the example calculations.

		DHI	DNI	GHI			
	W/m2	126	836	789			
	in×lbf/s / in^2	0.71946	4.77356	4.50519			
			°F	°R			
		Environment Temp	91.5	551.2			
		Sky Temp, BLAST model	80.7	540.4			
		Outer Wall Temp	110.9	570.6			
		Wall3	SS	Insulation	Plastic	Natural Conv	
		Surface Area, A	30952.75	30952.75	30952.75	A4	30952.75
		Thickness, L	0.25	2.5	0.25	HTCin, 2.5	0.00793
		Conductivity, K	2.03577	5.00E-03	2.38E-02		
		Resistance, R	0.000004	0.016167	0.00034	R4	0.004074
Side_wall_sun		Radiation of outer wall	Quantity	Unit			
		SB constant	3.09E-11	in×lbf/(s×in^2×°F^4)			
		Emissivity	0.5				
		Area	30952.75	in^2			
		Radiative heat	9898.0	in×lbf/s			
		Incident angle factor	0.60				
		Solar Radiation Flux, 798W/m^2	3.599473374	in×lbf/s / in^2			
		Absorptivity	0.5				
		Solar Radiation	55706.8	in×lbf/s			
		Convection at outer wall	Quantity	Unit			
		HTC, 23 W/m2K, 1.9m/s speed	0.073	in×lbf/(s×in^2×°F)			
		Convection heat	43822.2	in×lbf/s			
		Conduction into cab	Quantity	Unit			
		Total Resistance, R	0.020585	F/(in×lbf/s)			
		Cab air Temp	70	F			
		Conduction heat	1986.6	in×lbf/s			
		Ti	78.1				
		Heat Balance	-0.000040				

Appendix C-1. Sidewall in the sun calculations

(a) Solar radiation into the outer wall:

Solar Radiation = Solar radiation flux * Area * Absorptivity

Solar Radiation Flux = DNI * incident angle factor + DHI = 3.6 in-lbf/s/in^2

Area = 30,952.75 in^2

Absorptivity = 0.5

DNI and DHI are the components of solar radiation obtained from the historical data of solar radiation for the test date at the test location.

(b) Radiation of outer wall into the surroundings:

Radiative Heat = Stefan-Boltzmann constant * Emissivity * Area * (Outer wall temp^4 – Sky temp^4)

Stefan-Boltzmann constant = 3.09e-11 in-lbf/(s-in^2- °F^4)

Emissivity = 0.5

Area = 30,952.75 in^2

Sky temp = 540.4 °R (obtained from BLAST model)

Outer temp = 570.6 °R = 110.9 °F (calculated by using goal seek in excel spread sheet)

(c) Convection of outer wall into the surroundings:

Convection heat = Heat Transfer Coefficient * Area * (Outer wall temp – Environment temp)

Heat transfer coefficient = 0.073 in-lbf/(s-in^2- °F)

Area = 30,952.75 in^2

Outer temp = 570.6 °R = 110.9 °F (calculated by using goal seek in excel spread sheet)

Environment temp = 91.5 °F

(d) Conduction into the car:

Conduction heat = (Outer wall temp – Cab air temp) / Total resistance

Outer temp = 570.6 °R = 110.9 °F (calculated by using goal seek in excel spread sheet)

Cab air temp = 70 °F

Total resistance = resistance of steel outer shell + resistance of insulation + resistance of plastic + resistance due to natural convection right next to the wall

Resistance for each layer is calculated using the corresponding thickness, surface area and conductivity values.

The following heat balance equation is considered to compute the outer wall temperature.

Heat balance = Solar Radiation – Radiative heat – Convection heat – Conduction heat

The goal seek feature in the Excel spreadsheet is used to make this heat balance "0" by changing the outer wall temperature, and the resultant outer wall temperature and the corresponding conduction heat is noted from each of the walls.

The effect of seats and other structural components present in the car is considered, to calculate the distribution of heat required to heat those structural components and that required to heat the cabin air.[1] Deep thermal mass is defined as the overall thermal inertia of all objects other than air present inside the cabin. These objects include the seat structures, the dash and the dash components etc. which are combined with the cabin air in the lumped model. Deep thermal mass

[1] SAE International. "Comprehensive Modeling of Vehicle Air Conditioning Loads Using Heat Balance Model." Report No. 2013-01-1507. April 8, 2013.

in this reference literature is 5,600 J/K for one row of seats. For the car under consideration, there are 12 rows of seats. Hence, the deep thermal mass is considered as 12*5,600 J/K or 33,0428 in-lbf/ °F.

Air thermal mass is calculated as air density * specific heat * volume = 427,572 in-lbf/ °F

From this, it is calculated that 56 percent of the conduction heat calculated from the one-dimensional model will be heating the cabin air whereas the other 44 percent of the heat will be heating the seats and other structural components inside the car.

The heat transfer is calculated for every 1 minute from the one-dimensional model, to account for the reduced rate of heat transfer with the increase in the interior temperature. This calculated heat transfer through conduction into the car from all the structures was summed up and multiplied by 0.56 (for the air) and is given as input flux for the CFD model.

The spreadsheet with the calculation for all the structures is provided below.

Wall

	DHI	DNI	GHI
W/m2	126	836	789
in×lbf/s / in^2	0.71946	4.77356	4.50519

	°F	°R
Environment Temp	91.5	551.2
Sky Temp, BLAST model	80.7	540.4
Outer Wall Temp	110.9	570.6

Wall3	SS	Insulation	Plastic	Natural Conv	
Surface Area, A	30952.75	30952.75	30952.75	A4	30952.75
Thickness, L	0.25	2.5	0.25	HTCin, 2.5W/m2K	0.00793
Conductivity, K	2.03577	5.00E-03	2.38E-02		
Resistance, R	0.000004	0.016167	0.00034	R4	0.004074

Side_wall_sun

Radiation of outer wall	Quantity	Unit
SB constant	3.09E-11	in×lbf/(s×in^2×°F^4)
Emissivity	0.5	
Area	30952.75	in^2
Radiative heat	9898.0	in×lbf/s

Incident angle factor	0.60	
Solar Radiation Flux, 798W/m^2	3.599473374	in×lbf/s / in^2
Absorptivity	0.5	
Solar Radiation	55706.8	in×lbf/s

Convection at outer wall	Quantity	Unit
HTC, 23 W/m2K, 1.9m/s speed	0.073	in×lbf/(s×in^2×°F)
Convection heat	43822.2	in×lbf/s

Conduction into cab	Quantity	Unit
Total Resistance, R	0.020585	F/(in×lbf/s)
Cab air Temp	70	F
Conduction heat	1986.6	in×lbf/s
Ti	78.1	

Heat Balance	-0.000040	
Total conduction heat	8431.9	

	Air density	1.12E-07	1.225kg/m^3			
	Air specific heat	8.65E+05	1000 J/kg-K			
	Air Volume	4400000		Air	Seats	0
	Heat required for 1F raise	7.580E+05	in×lbf	427572.2	330427.9	90
	Heat required for 7F raise	5.306E+06	in×lbf	56%	44%	180
	Time required for 1F	1.50	min			270
	Time required for 7F	10.49	min			360
						450
SAE Ref. below	Deep Thermal Mass (DTM) - 1 row of seats	5600	J/K			540
	DTM for 24 seats (12 rows)	67200	J/K			630
1	J/K	4.91708	in×lbf/°F			
	DTM for 24 seats (12 rows)	330427.8507	in×lbf/°F			

SAE International

Comprehensive Modeling of Vehicle Air Conditioning Loads Using Heat Balance Method	2013-01-1507 Published 04/08/2013
Mohammad Ali Fayazbakhsh and Majid Bahrami Simon Fraser University	

doi:10.4271/2013-01-1507

Table 3. Specifications for the first simulated driving condition.

Specification	Value
Date	July 21, 2012
Local Time	13:00 to 16:00
Location	Houston, Texas
Driver Height, Weight	1.7 *m*, 70 *kg*
Passenger Height, Weight	1.6 *m*, 55 *kg*
Ventilation Flow	0.01 m^3/s (21.2 *CFM*)
Ground Reflectivity	0.2
Ambient Temperature	34.4°*C*
Initial Cabin Temperature	80°*C*
Ambient Relative Humidity	70%
Cabin Relative Humidity	50%
Comfort Temperature	23°*C*
Pull-Down Time	600 *s*
Deep Thermal Mass	5600 *J/K*

Each thermal load is calculated assuming a quasi-steady-state condition. Load calculations are performed at time steps during the simulation period of interest, and after every time step, all the load components are algebraically summed up and the new cabin air temperature and surface element temperatures are calculated as

$$\Delta T_i = \frac{\dot{Q}_{Tot}}{m_a c_a + DTM}\Delta t$$
$$\Delta T_s = \frac{\dot{Q}_s}{m_s c_s}\Delta t \qquad (2)$$

where ΔT_i and ΔT_s are the change in the cabin and surface element temperatures at the current time step. *DTM* is the sum of all the deep thermal masses *i.e.* the overall thermal inertia of all objects other than air present inside the cabin. These objects include the seat structures, the dash, the dash components, etc. which are combined with the cabin air in the lumped model. Δt is the time step, m_a is the cabin air mass and c_a is the air specific heat. m_s and c_s are the mass and specific heat of each of the surface elements and $\dot{Q}_s = \dot{Q}_{s,Rad} + \dot{Q}_{s,Amb}$ is the net heat gain by a surface element consisting of the heat gain by radiation, $\dot{Q}_{s,Rad}$, and the heat gain from ambient, $\dot{Q}_{s,Amb}$.

Angles

Stainless Steel thickness	0.25
Insulation thickness - walls	2.5
ABS plastic thickness	0.25
Insulation thickness - roof	1.5

	°F	°R
Environment Temp	91.5	551.2
Sky Temp, BLAST model	80.7	540.4
Outer Wall Temp	96.5	556.2

Wall2	SS	Insulation	Plastic	Natural Conv	
Surface Area, A	11000	11000	11000	A4	11000
Thickness, L	0.25	2.5	0.25	HTCin, 2.5W/m2K	0.00793
Conductivity, K	2.03577	5.00E-03	2.38E-02		
Resistance, R	0.000011	0.045493	0.000956	R4	0.011464

Backwall

Radiation of outer wall	Quantity	Unit
SB constant	3.08746E-11	in×lbf/(s×in^2×°F^4)
Emissivity	0.5	
Area	11000	in^2
Radiative heat	1768.7	in×lbf/s

Incident angle factor	0.09	
Solar Radiation Flux, 798W/m^2	1.134276985	in×lbf/s / in^2
Absorptivity	0.5	
Solar Radiation	6238.5	in×lbf/s

Convection at outer wall	Quantity	Unit
HTC, 23 W/m2K, 1.9m/s speed	0.073	in×lbf/(s×in^2×°F)
Convection heat	4012.4	in×lbf/s

Conduction into cab	Quantity	Unit
Total Resistance, R	0.057924	F/(in×lbf/s)
Cab air Temp	70	F

Conduction heat	457.4	in×lbf/s
Ti	75.2	

Heat Balance -0.000010

Surface area of Input face in CFD model 161331.434 in^2

70	8457.912	4770.933472	0.029572
71	8191.472	4620.640629	0.028641
72	7925.033	4470.347787	0.027709
73	7658.594	4320.054944	0.026778
74	7392.155	4169.762102	0.025846
75	7125.716	4019.469259	0.024914
76	6859.277	3869.176417	0.023983
77	6592.837	3718.883574	0.023051

	°F	°R
Environment Temp	91.5	551.2
Sky Temp, BLAST model	80.7	540.4
Outer Wall Temp	116.4	576.1

Wall1	SS	Insulation	Plastic	Natural Conv	
Surface Area, A	50000	50000	50000	A4	50000
Thickness, L	0.25	1.5	0.25	HTCin, 0.5W/m2K	0.001586
Conductivity, K	2.03577	5.00E-03	2.38E-02		
Resistance, R	0.000002	0.006005	0.000210324	R4	0.012610

Roof

Radiation of outer wall	Quantity	Unit
SB constant	3.08746E-11	in×lbf/(s×in^2×°F^4)
Emissivity	0.5	
Area	50000	in^2
Radiative heat	19199.3	in×lbf/s

Incident angle factor	0.79	
Solar Radiation Flux, 798W/m^2	4.503680515	in×lbf/s / in^2
Absorptivity	0.5	
Solar Radiation	112592.0	in×lbf/s

Convection at outer wall	Quantity	Unit
HTC, 23 W/m2K, 1.9m/s speed	0.073	in×lbf/(s×in^2×°F)
Convection heat	90927.7	in×lbf/s

Conduction into cab	Quantity	Unit
Total Resistance, R	0.018828	F/(in×lbf/s)
Cab air Temp	70	F
Conduction heat	2465.0	in×lbf/s
Ti	101.1	

Heat Balance -0.000055

	°F	°R
Environment Temp	91.5	551.2
Sky Temp, BLAST model	80.7	540.4
Outer Wall Temp	108.2	567.9

Windows	Glass	Natural Conv	
Surface Area, A	4247.25	A4	4247.25
Thickness, L	0.5	HTCin, 2.5W/m2K	0.00793
Conductivity, K	9.99E-02		
Resistance, R	0.001178	R4	0.029691

Windows

Radiation of outer wall	Quantity	Unit
SB constant	3.08746E-11	in×lbf/(s×in^2×°F^4)
Emissivity	0.5	
Area	4247.25	in^2
Radiative heat	1228.0	in×lbf/s

	°F	°R
Incident angle factor	0.60	
Solar Radiation Flux, 798W/m^2	3.599473374	in×lbf/s / in^2
Absorptivity	0.5	
Solar Radiation	7643.9	in×lbf/s

Convection at outer wall	Quantity	Unit
HTC, 23 W/m2K, 1.9m/s speed	0.073	in×lbf/(s×in^2×°F)
Convection heat	5178.4	in×lbf/s

Conduction into cab	Quantity	Unit
Total Resistance, R	0.030869	F/(in×lbf/s)
Cab air Temp	70	F
Conduction heat	1237.6	in×lbf/s
Ti	106.7	

Heat Balance	-0.000006	

	°F	°R
Environment Temp	91.5	551.2
Sky Temp, BLAST model	80.7	540.4
Outer Wall Temp	89.8	549.5

Wall4	SS	Insulation	Plastic	Natural Conv	
Surface Area, A	30952.75	30952.75	30952.75	A4	30952.75
Thickness, L	0.25	2.5	0.25	HTCin, 2.5W/m2K	0.00793
Conductivity, K	2.03577	5.00E-03	2.38E-02		
Resistance, R	0.000004	0.016167	0.00034	R4	0.004074

Side_wall_shade

Radiation of outer wall	Quantity	Unit
SB constant	3.09E-11	in×lbf/(s×in^2×°F^4)
Emissivity	0.5	
Area	30952.75	in^2
Radiative heat	2822.3	in×lbf/s

Incident angle factor	0.00	
Solar Radiation Flux, 798W/m^2	0	in×lbf/s / in^2
Absorptivity	0.5	
Solar Radiation	0.0	in×lbf/s

Convection at outer wall	Quantity	Unit
HTC, 23 W/m2K, 1.9m/s speed	0.073	in×lbf/(s×in^2×°F)
Convection heat	-3785.4	in×lbf/s

Conduction into cab	Quantity	Unit
Total Resistance, R	0.020585	F/(in×lbf/s)
Cab air Temp	70	F
Conduction heat	963.1	in×lbf/s
Ti	73.9	

Heat Balance	-0.000022	

	°F	°R
Environment Temp	91.5	551.2
Sky Temp, BLAST model	80.7	540.4
Outer Wall Temp	89.9	549.6

Floor	SS	Insulation	Wood	Natural Conv	
Surface Area, A	50000	50000	50000	A4	50000
Thickness, L	0.25	3	0.5	HTCin, 2.5W/m2K	0.00793
Conductivity, K	2.03577	5.00E-03	2.00E-02		
Resistance, R	0.000002	0.012010	0.0005	R4	0.002522

Floor

Radiation of outer wall	Quantity	Unit
SB constant	3.09E-11	in×lbf/(s×in^2×°F^4)
Emissivity	0.5	
Area	50000	in^2
Radiative heat	4587.8	in×lbf/s

	°F	°R
Incident angle factor	0.00	
Solar Radiation Flux, 798W/m^2	0	in×lbf/s / in^2
Absorptivity	0.5	
Solar Radiation	0.0	in×lbf/s

Convection at outer wall	Quantity	Unit
HTC, 23 W/m2K, 1.9m/s speed	0.073	in×lbf/(s×in^2×°F)
Convection heat	-5910.1	in×lbf/s

Conduction into cab	Quantity	Unit
Total Resistance, R	0.015035	F/(in×lbf/s)
Cab air Temp	70	F
Conduction heat	1322.3	in×lbf/s
Ti	73.3	

Heat Balance -0.000032

	l	41.69	0.727628		
	d	4.4	0.076794		
	h	5	0.087266		
	sinb	0.792746			
Solar altitude	b	52.4	0.915301		
Sun Zenith angle	tz	37.6			
Solar Azimuth	ph	171.8039	-0.98979	171.8039	0.9897859
ga2		81.8			
ga3		8.2			
	cos(t3)	0.60			
	t3	52.9	0.923131		
	Wall3				

	l	41.69	0.727628		
	d	4.4	0.076794		
	h	5	0.087266		
	sinb	0.792746			
Solar altitude	b	52.4	0.915301		
Sun Zenith angle	tz	37.6			
Solar Azimuth	ph	171.8039	-0.98979	171.8039	0.989786
ga2		81.8			
ga3		8.2			
	cos(t2)	0.09			
	t2	85.0	1.483788		
	Wall2				

	l	41.69	0.727628	
	d	4.4	0.076794	
	h	5	0.087266	
	sinb	0.792746		
Solar altitude	b	52.4	0.915301	
Sun Zenith angle	tz	37.6		
Solar Azimuth	ph	171.8039	-0.98979	171.8039
ga2		81.8		
ga3		8.2		
	cos(t1)	0.79		
	t1	37.6	0.655496	
	Wall1			

Windows-Area

Long windows	Length	48.5
	Height	20.5
	Area	994.25
Number of long windows		4
Narrow window		11.5
		23.5
	Area	270.25
Number of long windows		1
Total area of windows		4247.25

Abbreviations and Acronyms

ACRONYMS	EXPLANATION
AC	Air Conditioning
CFD	Computational Fluid Dynamics
FRA	Federal Railroad Administration
HEP	Head-End Power
HVAC	Heating Ventilation and Air Conditioning
hp	Horsepower
HMI	Human-Machine Interface
LBS	Least Significant Bit
Modbus RTU	Modbus Remote Terminal Unit
MBS	Most Significant Bit
NICTD	North Indiana Commuter Transportation District
PRIIA	Passenger Rail Investment and Improvement Act
PLC	Programmable Logic Controller
RTU	Remote Terminal Unit
RTD	Resistance Temperature Detector
SA	Sharma & Associates, Inc.
S/N	Subnet/Node (Address)
T/C	Thermocouple
VAC	Volt Alternating Current